VPI-IHEP-95-08
TUIMP-TH-95/66
MSUHEP-50620
August, 1995

SENSITIVITY OF THE LHC TO ELECTROWEAK SYMMETRY BREAKING: EQUIVALENCE THEOREM AS A CRITERION

Hong-Jian He [(a)], **Yu-Ping Kuang** [(b)], **C.–P. Yuan** [(c)]

[(a)] *Department of Physics and Institute of High Energy Physics*
Virginia Polytechnic Institute and State University
Blacksburg, Virginia 24061-0435, USA

[(b)] *CCAST (World Laboratory), P.O.Box 8730, Beijing 100080, China*
Institute of Modern Physics, Tsinghua University, Beijing 100084, China *

[(c)] *Department of Physics and Astronomy, Michigan State University*
East Lansing, Michigan 48824, USA

Abstract

Based upon our recent study on the intrinsic connection between the longitudinal weak-boson scatterings and probing the electroweak symmetry breaking (EWSB) mechanism, we reveal the profound physical content of the Equivalence Theorem (ET) as being able to discriminate physical processes which are sensitive/insensitive to probing the EWSB sector. With this physical content of the ET as a criterion, we analyze the complete set of the bosonic operators in the electroweak chiral Lagrangian and systematically classify the sensitivities to probing all these operators at the CERN LHC via the weak-boson fusion in $W^{\pm}W^{\pm}$ channel. This is achieved by developing a precise power counting rule (a generalization from Weinberg's counting method) to *separately* count the power dependences on the energy E and all relevant mass scales.

PACS number(s): 11.30.Qc, 11.15.Ex, 12.15.Ji, 14.70.–e

*Mailing address.

1. Introduction

Despite the astonishing success of the Standard Model (SM) over the years, its scalar part, the electroweak symmetry breaking (EWSB) sector, remains as the greatest mystery. Due to Veltman's screening theorem [1], the current low energy data, allowing the SM Higgs boson mass to range from 60 GeV to about 1 TeV, tell us little about the EWSB mechanism. It is therefore important to probe *all possible EWSB mechanisms, either weakly or strongly interacting* as long as the light Higgs particle remains undetected.

While the transverse components V_T^a of $W^\pm,\ Z^0$ are irrelevant to the EWSB mechanism, the longitudinal weak-bosons ($V_L^a = W_L^\pm,\ Z_L^0$), as the products of the spontaneously symmetry-breaking mechanism, are expected to be sensitive to probing the EWSB sector. However, even for the strongly coupled case, studying the V_L-scatterings does not guarantee probing the EWSB sector in a sensitive and unambiguous way because the spin-0 Goldstone bosons (GB's) are invariant under the proper Lorentz transformations, while, on the contrary, both V_L and V_T are Lorentz non-invariant (LNI). After a Lorentz transformation, the V_L component can mix with or even turn into a pure V_T. Thus a conceptual and fundamental ambiguity arises: How can the LNI V_L-amplitudes be used to probe the EWSB sector of which the physical mechanism should clearly be independent of the choices of the Lorentz frames? This motivated our recent precise formulation of the electroweak Equivalence Theorem (ET) in Ref. [2]. In the high energy region ($E \gg M_W$), the ET provides a quantitative relation between the V_L-amplitude and the corresponding GB-amplitude [3, 4, 2]; the former is physically measurable while the latter carries information about the EWSB sector. Hence, the ET allows us to probe the EWSB sector by relating it to the V_L-scattering experiments. As will be shown later, the *difference* between the V_L- and GB-amplitudes is intrinsically related to the ambiguous LNI part of the V_L-scattering which has the same origin as the V_T-amplitude, and is thus insensitive to probing the EWSB sector. When the LNI contributions can be safely ignored and the Lorentz invariant (LI) scalar GB-amplitude dominates the experimentally measured V_L-amplitudes, the physical V_L-scatterings can then sensitively and unambiguously probe the EWSB mechanism. Since the ratio of the LNI contributions to the LI GB-amplitude is *process-dependent*, it can thus determine the sensitivities of various scattering processes to probing the EWSB sector.

At the scale below new heavy resonances, all the effects due to the EWSB can be parametrized by a complete set of effective operators in the electroweak chiral Lagrangian (EWCL). Without experimental observation of any new light resonance in the EWSB sector, this effective field theory approach provides an elegant way to generally parametrize all possible new physics effects in the low energy region and is thus *complementary* to those specific model buildings. In this paper, we take an economical and conservative viewpoint and adopt the EWCL approach for our investigation. We shall concentrate on studying the bosonic operators among which the leading order operators are universal (independent of models of EWSB) and all the model-dependent effects are described by the next-to-leading-order operators in the EWCL. We show in this paper that for a given process the ratio of the LNI contributions in the V_L-amplitude to the scalar GB-amplitude varies for different effective operators. *Therefore, this ratio can be used to discriminate sensitivities to the next-to-leading-order effective operators as well as to the scattering processes for probing the EWSB sector.* The smaller this ratio, the more sensitive a process will be to an operator. We shall classify the sensitivities to all these effective operators at the CERN Large Hadron Collider (LHC). Through this analysis, we show that the ET is not just a technical tool in computing V_L-amplitudes via GB-amplitudes, *as a criterion, it has an even more profound physical content for being able to discriminate sensitivities to different effective operators via different processes for probing the EWSB mechanism.*

This paper is organized as follows. We first formulate the ET as a criterion for probing the EWSB mechanism in Sec. 2, and derive a precise electroweak power counting rule for the EWCL formalism in Sec. 3. Then, in Sec. 4, we classify the sensitivities of all effective operators at the level of the S-matrix elements. Finally we analyze, in Sec. 5, the probe of the EWSB at the LHC (a pp collider with $\sqrt{S} = 14\,\text{TeV}$) via weak-boson scatterings. Conclusions are given in Sec. 6. Also, a detailed analysis on the the validity of the ET in some special kinematic regions and its implication in probing the EWSB sector is presented in the Appendix.

2. Formulating the ET as a Criterion for Probing the EWSB

Starting from the Slavnov-Taylor identity [3, 4] $\quad < 0\,|F_0^{a_1}(k_1)\cdots F_0^{a_n}(k_n)\,\Phi_\alpha|\,0 >$

$= 0$ [a] and making a rigorous Lehmann-Symanzik-Zimmermann (LSZ) reduction for the external F^a-lines, we derived the following general identity for the renormalized S-matrix elements:[b]

$$T[V_L^{a_1},\cdots,V_L^{a_n};\Phi_\alpha] = C\cdot T[-i\pi^{a_1},\cdots,-i\pi^{a_n};\Phi_\alpha] + B \quad , \tag{2.1}$$

$$\begin{aligned} C &\equiv C_{mod}^{a_1}\cdots C_{mod}^{a_n} \ , \\ B &\equiv \textstyle\sum_{l=1}^{n}\big(C_{mod}^{a_{l+1}}\cdots C_{mod}^{a_n} T[v^{a_1},\cdots,v^{a_l},-i\pi^{a_{l+1}},\cdots,-i\pi^{a_n};\Phi_\alpha] \\ &\qquad + \text{ permutations of } v'\text{s and } \pi'\text{s } \big) \ , \\ v^a &\equiv v^\mu V_\mu^a \ , \quad v^\mu \equiv \epsilon_L^\mu - k^\mu/M_a = O(M_a/E) \ , \quad (M_a = M_W, M_Z) \ , \end{aligned} \tag{2.1a,b,c}$$

where π^a's are GB fields; and the finite constant modification factor C_{mod}^a has been systematically studied in Ref. [4], which can be exactly simplified as unity in some renormalization schemes [5]. Without losing generality [2], let us assume that Φ_α contains some physical scalars, photons, or no field at all. From (2.1), the LNI V_L-amplitude can be decomposed into two parts: the 1st part is $C\cdot T[-i\pi;\Phi_\alpha]$ which is LI; the 2nd part is the v_μ-suppressed B-term which is LNI because it contains the external spin-1 V_μ-field(s). Such a decomposition shows the *essential difference* between the V_L- and the V_T-amplitudes. The former contains a LI GB-amplitude that can yield a large V_L-amplitude in the case of strongly coupled EWSB sector. We note that only the LI part of the V_L-amplitude is sensitive to probing the EWSB sector, while its LNI part contains a significant *Lorentz-frame-dependent* B-term and is therefore not sensitive to the EWSB mechanism. Thus, for a sensitive and unambiguous probe of the EWSB, we must find conditions that the LI GB-amplitude dominates the V_L-amplitude and the LNI B-term can be ignored. It is clear that one can technically improve the prediction for the V_L-amplitude from the RHS of (2.1) by including the complicated B-term (or part of B) [6], but this is not an improvement of the equivalence between the V_L- and GB-amplitudes. *The physical content of the ET is essentially independent of how to compute the V_L-amplitude. It is the LI GB-amplitude that really matters for sensitively probing the EWSB sector.*

From a detailed analysis on the LNI V_L-amplitude, we can estimate the B-term as [2]

$$B \approx O(\frac{M_W^2}{E_j^2})T[-i\pi^{a_1},\cdots,-i\pi^{a_n};\Phi_\alpha] + O(\frac{M_W}{E_j})T[V_{T_j}^{a_{r_1}},-i\pi^{a_{r_2}},\cdots,-i\pi^{a_{r_n}};\Phi_\alpha] \quad . \tag{2.2}$$

[a] Here, F_0^a is the bare gauge fixing function and Φ_α denotes other possible physical in/out states.

[b] See the second paper by H.-J. He, Y.-P. Kuang and X. Li in Ref. [4].

We see that the condition $E_j \sim k_j \gg M_W,\ (j = 1, 2, \cdots, n)$ *for each external longitudinal weak-boson* is *necessary* for making the B-term (and its Lorentz variation) to be much smaller than the GB-amplitude. This also precisely defines the *safe Lorentz frames* in which the LNI B-term can be ignored, cf. (2.3). In conclusion, we give our general and precise formulation of the ET as follows:

$$T[V_L^{a_1}, \cdots, V_L^{a_n}; \Phi_\alpha] = C \cdot T[-i\pi^{a_1}, \cdots, -i\pi^{a_n}; \Phi_\alpha] + O(M_W/E_j\text{−suppressed}), \tag{2.3}$$

$$\begin{array}{l} E_j \sim k_j \gg M_W, \qquad (\ j = 1, 2, \cdots, n\ )\ \ ; \\ B \ll C \cdot T[-i\pi^{a_1}, \cdots, -i\pi^{a_n}; \Phi_\alpha]\ \ , \end{array} \tag{2.3a, b}$$

where (2.3a,b) *are the precise conditions for ignoring the LNI B-term to validate the equivalence in* (2.3). We emphasize that, in principle, the complete set of diagrams (including those with internal gauge boson lines) has to be considered when calculating $T[-i\pi^{a_1}, \cdots, -i\pi^{a_n}; \Phi_\alpha]$. If not, this equivalence might not manifest for forward or backward scatterings for processes involving t- or u- channel diagram. A detailed discussion on this point is given in the Appendix.

The amplitude T, to a finite order, can be written as $T = \sum_{\ell=0}^{N} T_\ell = \sum_{\ell=0}^{N} \bar{T}_\ell \alpha^\ell$ in the perturbative calculation. Let $T_0 > T_1, \cdots, T_N \geq T_{\min}$, where $T_{\min} = \{T_0, \cdots, T_N\}_{\min}$, then the condition (2.3b) implies

$$\begin{array}{rl} B & \approx O(\frac{M_W^2}{E_j^2})\, T_0[-i\pi^{a_1}, \cdots, -i\pi^{a_n}; \Phi_\alpha] + O(\frac{M_W}{E_j})\, T_0[V_{T_j}^{a_{r_1}}, -i\pi^{a_{r_2}}, \cdots, -i\pi^{a_{r_n}}; \Phi_\alpha] \\ & \ll T_{\min}[-i\pi^{a_1}, \cdots, -i\pi^{a_n}; \Phi_\alpha]\ \ . \end{array} \tag{2.4}$$

Note that *the above formulation of the ET discriminates processes which are insensitive to probing the EWSB sector when either* (2.3a) *or* (2.3b) *fails.* Furthermore, *as a physical criterion, the condition (2.4) determines whether or not the corresponding V_L-scattering process in (2.3) is sensitive to probing the EWSB sector to the desired precision in perturbative calculations.*

From (2.2) or the LHS of (2.4) and the precise electroweak power counting rule (to be discussed in Sec. 3), we can easily estimate the *largest* and *model-independent* B-term to be $B_{\max} = O(g^2) f_\pi^{4-n}$ in the EWCL formalism,[c] which comes from the n-particle pure V_L-amplitude. It is crucial to note that $B_{\max}$ is of the same order of magnitude as

[c]This is also true for the heavy Higgs SM.

the leading V_T-amplitude:

$$B_{\max} \approx T_0[V_T^{a_1}, \cdots, V_T^{a_n}] = O(g^2) f_\pi^{4-n} \quad . \tag{2.5}$$

Since both the largest B-term and the leading V_T-amplitude are of $O(g^2)$, they are therefore irrelevant to the EWSB mechanism as pointed out in the above analysis. Thus, *(2.4) and (2.5) provide useful criteria for discriminating physical processes which are sensitive, marginally sensitive, or insensitive to the EWSB sector.*

3. Generalized Precise Power Counting for the Electroweak Chiral Lagrangian

In this section, we generalize Weinberg's counting method [7] and develop a precise counting rule for the EWCL in the energy region $M_W, m_t \ll E \ll \Lambda$,[d] where the effective cutoff Λ is the upper limit of E at which the EWCL formalism ceases to be applicable. In this work we shall assume that the EWSB sector does not contain any new resonance below the scale $\Lambda \simeq 4\pi f_\pi \simeq 3.1\,\text{TeV}$. We want to *separately* count the power dependences of the amplitudes on the energy E, the cutoff scale Λ of the EWCL and the Fermi scale $f_\pi = 246\,\text{GeV}$ ($\sim M_W, m_t$).[e] This is *crucial* for estimating the order of magnitude of an amplitude at any given order of perturbative calculation. For example, an amplitude of $O(E^2/f_\pi^2)$ differs by an order of magnitude from an amplitude of $O(E^2/\Lambda^2)$ in spite that they have the same E-dependence. Since the weak-boson mass $M_W = g f_\pi/2$ and the fermion mass $m_f = y_f f_\pi/\sqrt{2}$, we can count them in powers of the coupling constants g and y_f and the vacuum expectation value f_π. The $SU(2)$ weak gauge coupling g and the top quark Yukawa coupling y_t are close to 1 and thus will not significantly affect the order of magnitude estimates. The electromagnetic $U(1)_{em}$ coupling $e = g \sin\theta_W$ is smaller than g by a factor of 2. The Yukawa couplings of all light SM fermions other than the top quark are negligibly small. In our following precise counting rule, the dependences on coupling constants g, g'(or e) and y_t are included, while all the light fermion Yukawa couplings [y_f ($\neq y_t$) $\ll 1$] are ignored.

[d] The generalizations of Weinberg's counting method to the light Higgs SM and heavy Higgs SM are given in Ref. [8].

[e] This is essentially different from the previous counting for the heavy Higgs SM where only the *sum* of the powers of E and m_H has been counted [9].

The original Weinberg's power counting rule was derived only for counting the energy dependence in the un-gauged nonlinear σ-model as a description of low energy QCD interaction [7]. The *general* features of Weinberg's counting method are: (i). The total dimension D_T of an S-matrix element T is determined by the number of external lines and the space-time dimension; (ii). Assume that all mass poles in the internal propagators of T are much smaller than the typical energy scale E of T , then the total dimension D_m of the E-independent coupling constants included in T can be directly counted according to all types of vertices it contains. Hence, the total E-power D_E for T is given by $D_E = D_T - D_m$.

Here, we shall make a natural generalization of Weinberg's power counting method for the EWCL in which, except the light SM gauge bosons, fermions and would-be GB's, all possible heavy fields have been integrated out. It is clear that in this case the above conditions (i) and (ii) are satisfied. The total dimension of an L-loop S-matrix element T is

$$D_T = 4 - e \quad , \tag{3.1}$$

where $e = e_B + e_F$, and e_B (e_F) is the number of external bosonic (fermionic) lines. Here the dimensions of the external spinor wave functions are already included in D_T. For external fermionic lines, we only count the SM fermions with masses $m_f \leq m_t \sim O(M_W) \ll E$. So the spinor wave function of each external fermion will contribute an energy factor $E^{1/2}$ for $E \gg m_f$, where the spinor wave functions are normalized as $\bar{u}(p,s)u(p,s') = 2m_f\delta_{ss'}$, etc. Let us label the different types of vertices by an index n. If the vertex of type n contains b_n bosonic lines, f_n fermionic lines and d_n derivatives, then the dimension of the E-independent effective coupling constant in T is

$$D_m = \sum_n \mathcal{V}_n(4 - d_n - b_n - \frac{3}{2}f_n) \quad , \tag{3.2}$$

where $\mathcal{V}_n$ is the number of vertices of type n. Let i_B and i_F be the numbers of internal bosonic and fermionic lines, respectively. (i_B also includes possible internal ghost lines.) Define $i = i_B + i_F$, we have, in addition, the following general relations

$$\sum_n b_n\mathcal{V}_n = 2i_B + e_B \quad , \qquad \sum_n f_n\mathcal{V}_n = 2i_F + e_F \quad , \qquad L = 1 + i - \sum_n \mathcal{V}_n \quad . \tag{3.3}$$

Among the external vector-boson lines, each V_L-line contains a polarization vector ϵ_L which is of $O(E/M_W)$, and each v_μ defined in (2.1c) is of $O(M_W/E)$. Let e_L and e_v

denote the numbers of external V_L and v_μ lines, respectively. Then from (3.1), (3.2) and (3.3), the leading energy power in T is

$$D_E \ = D_T - D_m + e_L - e_v \ = 2L + 2 + \sum_n \mathcal{V}_n(d_n + \frac{1}{2}f_n - 2) + e_L - e_v \ . \tag{3.4}$$

This is just the Weinberg's counting rule [7] in its generalized form with the gauge boson, ghost and fermion fields and possible v_μ-factors included.[f]

A subtle point should be noted. To show this, we take the $V_LV_L \to V_LV_L$ scattering amplitude as an example, in which $e_L = 4$ and $e_v = e_F = 0$. To the lowest order of the EWCL, the leading powers of E in $T[V_L^{a_1}, \cdots, V_L^{a_4}]$ and $T[\pi^{a_1}, \cdots, \pi^{a_4}]$ are E^4 and E^2, respectively. This tells us that the naive power counting for V_L-amplitude only gives the leading E-power for individual graphs. It does not reflect the fact that gauge invariance causes the cancellations of the E^4-terms, and leads to the final E^2-dependence of the whole V_L-amplitude. Thus the naive power counting of the V_L-amplitudes does not give the correct answer. However, the power counting of GB-amplitude does give the correct E-dependence because, unlike in the V_L-amplitudes, there is generally no large E-power cancellations in the GB-amplitudes. Therefore based on our ET identity (2.1) the correct counting in powers of E for the V_L-amplitude can be given by counting the corresponding GB-amplitude plus the B-term. So in what follows, we shall not directly count the E-dependence in diagrams with external longitudinal weak-boson lines. They will be counted through counting the RHS of the ET identity in (2.1). We shall therefore drop the e_L term in (3.4), and *make the convention that the number of external vector-boson lines e_V counts only the number of external V_T-lines and photon lines.*

In the following, we further develop a precise power counting rule for the EWCL to separately count the dependence of S-matrix elements on energy (E), cutoff scale (Λ) of the effective Lagrangian and vacuum expectation value (f_π). This separate counting on the powers of E, Λ and f_π is important for estimating contributions to scattering amplitudes from various effective operators in the Lagrangian. In general, the EWCL can be constructed as [10, 11]:

$$\mathcal{L}_{eff} \ = \sum_n \ell_n \frac{{f_\pi}^{r_n}}{\Lambda^{a_n}} \mathcal{O}_n(W_{\mu\nu}, B_{\mu\nu}, D_\mu U, U, f, \bar{f}) = \mathcal{L}_G + \mathcal{L}_S + \mathcal{L}_F \tag{3.5}$$

[f](3.4) is clearly valid for any gauge theory satisfying the above conditions (i) and (ii).

where

$$D_\mu U = \partial_\mu U + ig\mathbf{W}_\mu U - ig' U\mathbf{B}_\mu \ ,$$

$$U = \exp[i\tau^a\pi^a/f_\pi] \ , \quad \mathbf{W}_\mu \equiv W_\mu^a \frac{\tau^a}{2} \ , \quad \mathbf{B}_\mu \equiv B_\mu \frac{\tau^3}{2} \ .$$

$f(\bar{f})$ is the SM fermion with mass $m_f \leq O(m_t) \simeq O(M_W)$. $\mathcal{L}_G$, $\mathcal{L}_S$ and $\mathcal{L}_F$ denote gauge boson kinetic terms, scalar boson interaction terms (containing GB self-interactions and gauge-boson-GB interactions), and fermion interaction terms, respectively. For clearness, we have factorized out the dimensionful parameters f_π and Λ in the coefficients so that the dimensionless factor $\ell_i \sim O(1)$.[g] We note that f_π and Λ are the two essential scales in any effective Lagrangian that describes the spontaneously broken symmetry. The former determines the symmetry breaking scale while the latter determines the scale at which new resonance(s) besides the light fields (such as the SM weak bosons, would-be Goldstone bosons and fermions) may appear. For the non-decoupling scenario, the effective cutoff scale Λ cannot be arbitrarily large. It is $\Lambda = \min(M_{SB}, 4\pi f_\pi)$, where M_{SB} is the mass of the lightest new resonance, and $\Lambda \simeq 4\pi f_\pi$ [12] for the case without new resonance in the EWSB sector. In (3.5), $r_n = 4 + a_n - D_{\mathcal{O}_n}$, where $D_{\mathcal{O}_n} = \dim(\mathcal{O}_n)$. For the bosonic part of EWCL, we have [10]:

[g] This makes our definitions of the ℓ_i's different from the α_i's in Ref. [10] by a factor of $(f_\pi/\Lambda)^2$.

$$
\begin{aligned}
\mathcal{L}_G &= -\tfrac{1}{2}\mathrm{Tr}(\mathbf{W}_{\mu\nu}\mathbf{W}^{\mu\nu}) - \tfrac{1}{4}B_{\mu\nu}B^{\mu\nu} \ , \\
\mathcal{L}_S &= \mathcal{L}^{(2)} + \mathcal{L}^{(2)\prime} + \sum_{n=1}^{14}\mathcal{L}_n \ , \\
\mathcal{L}^{(2)} &= \tfrac{f_\pi^2}{4}\mathrm{Tr}[(D_\mu U)^\dagger (D^\mu U)] \ , \\
\mathcal{L}^{(2)\prime} &= \ell_0(\tfrac{f_\pi}{\Lambda})^2 \ \tfrac{f_\pi^2}{4}[\mathrm{Tr}(\mathcal{T}\mathcal{V}_\mu)]^2 \ , \\
\mathcal{L}_1 &= \ell_1(\tfrac{f_\pi}{\Lambda})^2 \ \tfrac{gg'}{2}B_{\mu\nu}\mathrm{Tr}(\mathcal{T}\mathbf{W}^{\mu\nu}) \ , \\
\mathcal{L}_2 &= \ell_2(\tfrac{f_\pi}{\Lambda})^2 \ \tfrac{ig'}{2}B_{\mu\nu}\mathrm{Tr}(\mathcal{T}[\mathcal{V}^\mu, \mathcal{V}^\nu]) \ , \\
\mathcal{L}_3 &= \ell_3(\tfrac{f_\pi}{\Lambda})^2 \ ig\mathrm{Tr}(\mathbf{W}_{\mu\nu}[\mathcal{V}^\mu, \mathcal{V}^\nu]) \ , \\
\mathcal{L}_4 &= \ell_4(\tfrac{f_\pi}{\Lambda})^2[\mathrm{Tr}(\mathcal{V}_\mu\mathcal{V}_\nu)]^2 \ , \\
\mathcal{L}_5 &= \ell_5(\tfrac{f_\pi}{\Lambda})^2[\mathrm{Tr}(\mathcal{V}_\mu\mathcal{V}^\mu)]^2 \ , \\
\mathcal{L}_6 &= \ell_6(\tfrac{f_\pi}{\Lambda})^2[\mathrm{Tr}(\mathcal{V}_\mu\mathcal{V}_\nu)]\mathrm{Tr}(\mathcal{T}\mathcal{V}^\mu)\mathrm{Tr}(\mathcal{T}\mathcal{V}^\nu) \ , \\
\mathcal{L}_7 &= \ell_7(\tfrac{f_\pi}{\Lambda})^2[\mathrm{Tr}(\mathcal{V}_\mu\mathcal{V}^\mu)]\mathrm{Tr}(\mathcal{T}\mathcal{V}_\nu)\mathrm{Tr}(\mathcal{T}\mathcal{V}^\nu) \ , \\
\mathcal{L}_8 &= \ell_8(\tfrac{f_\pi}{\Lambda})^2 \ \tfrac{g^2}{4}[\mathrm{Tr}(\mathcal{T}\mathbf{W}_{\mu\nu})]^2 \ , \\
\mathcal{L}_9 &= \ell_9(\tfrac{f_\pi}{\Lambda})^2 \ \tfrac{ig}{2}\mathrm{Tr}(\mathcal{T}\mathbf{W}_{\mu\nu})\mathrm{Tr}(\mathcal{T}[\mathcal{V}^\mu, \mathcal{V}^\nu]) \ , \\
\mathcal{L}_{10} &= \ell_{10}(\tfrac{f_\pi}{\Lambda})^2\tfrac{1}{2}[\mathrm{Tr}(\mathcal{T}\mathcal{V}^\mu)\mathrm{Tr}(\mathcal{T}\mathcal{V}^\nu)]^2 \ , \\
\mathcal{L}_{11} &= \ell_{11}(\tfrac{f_\pi}{\Lambda})^2 \ g\epsilon^{\mu\nu\rho\lambda}\mathrm{Tr}(\mathcal{T}\mathcal{V}_\mu)\mathrm{Tr}(\mathcal{V}_\nu\mathbf{W}_{\rho\lambda}) \ , \\
\mathcal{L}_{12} &= \ell_{12}(\tfrac{f_\pi}{\Lambda})^2 \ 2g\mathrm{Tr}(\mathcal{T}\mathcal{V}_\mu)\mathrm{Tr}(\mathcal{V}_\nu\mathbf{W}^{\mu\nu}) \ , \\
\mathcal{L}_{13} &= \ell_{13}(\tfrac{f_\pi}{\Lambda})^2 \ \tfrac{gg'}{4}\epsilon^{\mu\nu\rho\lambda}B_{\mu\nu}\mathrm{Tr}(\mathcal{T}\mathbf{W}_{\rho\lambda}) \ , \\
\mathcal{L}_{14} &= \ell_{14}(\tfrac{f_\pi}{\Lambda})^2 \ \tfrac{g^2}{8}\epsilon^{\mu\nu\rho\lambda}\mathrm{Tr}(\mathcal{T}\mathbf{W}_{\mu\nu})\mathrm{Tr}(\mathcal{T}\mathbf{W}_{\rho\lambda}) \ ,
\end{aligned}
\tag{3.6}
$$

where $\mathbf{W}_{\mu\nu} = \partial_\mu\mathbf{W}_\nu - \partial_\nu\mathbf{W}_\mu - ig[\mathbf{W}_\mu, \mathbf{W}_\nu]$, $\mathcal{V}_\mu \equiv (D_\mu U)U^\dagger$, and $\mathcal{T} \equiv U\tau_3 U^\dagger$. There are fifteen next-to-leading-order effective operators among which there are twelve CP-conserving operators ($\mathcal{L}^{(2)\prime}, \mathcal{L}_{1\sim 11}$) and three CP-violating operators ($\mathcal{L}_{12\sim 14}$). Furthermore, the operators $\mathcal{L}_{6,7,10}$ violate custodial $SU(2)_C$ symmetry (even after g' being turned off) contrary to $\mathcal{L}_{4,5}$ which contain $SU(2)_C$-invariant pure GB interactions. The coefficients (ℓ_n's) of all the above operators are model-dependent and carry information about possible new physics beyond the SM. The dimension-2 custodial $SU(2)_C$-violating operator $\mathcal{L}^{(2)\prime}$ has a coefficient of $O((f_\pi/\Lambda)^2)$ since it is proportional to $\delta\rho \simeq O(m_t^2/(16\pi^2 f_\pi^2)) \simeq O((f_\pi/\Lambda)^2)$ for the top Yukawa coupling being of $O(1)$.

In the non-decoupling scenario [12, 13], all the coefficients for dimension-4 operators are suppressed by a factor $(f_\pi/\Lambda)^2 \simeq 1/(16\pi^2)$ because they arise from the derivative

expansion in $(D_\mu/\Lambda)^2$. After the small CP-violating effects from the Cabibbo-Kobayashi-Maskawa mixings are ignored in the lowest order fermionic operators contained in $\mathcal{L}_F$, all the one-loop level new divergences generated from $\mathcal{L}_G + \mathcal{L}_F + \mathcal{L}^{(2)}$ are thus CP-invariant. Therefore, the CP-violating operators $\mathcal{L}_{12\sim 14}$ are actually *decoupled* at this level, and their coefficients can have values significantly larger or smaller than that from the naive dimensional analysis [12]. Since the true mechanism for CP-violation remains un-revealed, we shall consider in this paper the coefficients $\ell_{12\sim 14}$ to be around of $O(1)$.

Consider the S-matrix element T at L-loop order. Since we are dealing with a spontaneously broken gauge theory which possesses a nonvanishing vacuum expectation value (f_π), T can always be written as $f_\pi^{D_T}$ times some dimensionless function of E, Λ, and f_π , etc. The E-power dependence has been given by our generalized Weinberg formula (3.4). Since the cutoff scale Λ in the EWCL is much larger than f_π (for $\Lambda/f_\pi \simeq 4\pi$), it is crucial to separately count Λ and f_π to correctly estimate the magnitude of an amplitude. The Λ-dependence in T can only come from two sources:

(i). From tree vertices: T contains $\mathcal{V} = \sum_n \mathcal{V}_n$ vertices, each of which contributes a factor $1/\Lambda^{a_n}$ so that the total factor from $\mathcal{V}$-vertices is $1/\Lambda^{\sum_n a_n}$;

(ii). From loop-level: Since each loop brings a factor $(1/4\pi)^2 \simeq (f_\pi/\Lambda)^2$, the total Λ-dependence from loop contribution is $1/\Lambda^{2L}$.

Hence the total Λ-dependence given by the above two sources is $1/\Lambda^{\sum_n a_n + 2L}$. From the above discussion, we conclude the following precise counting rule for T :

$$
\begin{aligned}
T &= c_T f_\pi^{D_T} \left(\frac{f_\pi}{\Lambda}\right)^{N_\mathcal{O}} \left(\frac{E}{f_\pi}\right)^{D_{E0}} \left(\frac{E}{\Lambda}\right)^{D_{EL}} \left(\frac{M_W}{E}\right)^{e_v} H(\ln E/\mu) \ , \\
N_\mathcal{O} &= \sum_n a_n \ , \qquad D_{E0} = 2 + \sum_n \mathcal{V}_n (d_n + \frac{1}{2} f_n - 2) \ , \qquad D_{EL} = 2L \ ,
\end{aligned}
\tag{3.7}
$$

where the dimensionless coefficient c_T contains possible powers of gauge couplings (g, g') and Yukawa couplings (y_f) from the vertices in T . H is a function of $\ln(E/\mu)$ which is insensitive to E. (Here μ denotes the relevant renormalization scale for loop calculations.) We note that because pure GB vertices contain the highest power of derivatives at each order of derivative expansion, (3.7) shows that the leading E-power dependence is always given by pure GB self-interacting graphs. The same conclusion holds

for pure V_L-scattering amplitudes since they can be decomposed into the corresponding GB-amplitudes plus the M_W/E-suppressed B-term [cf. (2.1)].

4. Classification of sensitivities at the level of S-matrix elements

Armed with the above counting rule (3.7), we can easily estimate the contributions from various effective operators in the EWCL to any scattering process such that we can systematically classify the sensitivities to the next-to-leading-order effective operators for probing the EWSB sector at the LHC. Our electroweak power counting analysis makes it possible to quickly grasp the overall semi-quantitative physical picture which provides useful guidance on selecting relevant operators and scattering processes to perform further detailed studies.

In this paper we shall concentrate on the high energy weak-boson scatterings. As shown in Ref. [14], for the non-resonance case (i.e. no new light resonance in the symmetry breaking sector) the most important scattering process for probing the EWSB sector is the same-charged channel: $W^\pm W^\pm \to W^\pm W^\pm$. In Tables 1a and 1b we estimate the contributions from the lowest order (model-independent) operators in $\mathcal{L}_0 \equiv \mathcal{L}_G + \mathcal{L}_F + \mathcal{L}^{(2)}$ up to one-loop and from all the next-to-leading-order (model-dependent) bosonic operators in (3.6) at tree-level for $W^\pm W^\pm \to W^\pm W^\pm$. For instance, the commonly discussed operators $\mathcal{L}_{4,5}$ contribute the model-dependent leading term of $O(\frac{E^2}{f_\pi^2}\frac{E^2}{\Lambda^2})$ to the $T[4W_L]$ amplitude, and the sub-leading term of $O(g\frac{E}{f_\pi}\frac{E^2}{\Lambda^2})$ to the $T[3W_L, W_T]$ amplitude. The model-independent and model-dependent contributions to various B-terms are summarized in Tables 2a and 2b, in which $B_\ell^{(i)}$ $(i = 0, \cdots, 3;\ \ell = 0, 1, \cdots)$ denotes the B-term from V_L-amplitudes containing $0, 1, 2, 3$ external V_T-lines, respectively. Here $B_0^{(i)}$ is obtained from the tree level and $B_1^{(i)}$ from the next-to-leading order. We see that the largest B-term is $B_0^{(0)}$ from the $4W_L$ amplitudes, as given in (2.5). The $B_0^{(0)}$, which is $O(g^2)$, is a model-independent constant containing only the SM gauge coupling constants. All the other B-terms are further suppressed by a factor of M_W/E or $(E/\Lambda)^2$, or a product of them.

From Tables 1∼2 and our recent exhaustive study [8] for $V^aV^b \to V^cV^d$ scatterings, we further classify in Table 3 the sensitivities to all the bosonic operators for probing

the EWSB sector directly (from pure GB interactions) or indirectly (from interactions suppressed by the SM gauge coupling constants). The classification is based on the following hierarchy in the power counting:

$$\frac{E^2}{f_\pi^2} \gg \frac{E^2}{f_\pi^2}\frac{E^2}{\Lambda^2},\ g\frac{E}{f_\pi} \gg g\frac{E}{f_\pi}\frac{E^2}{\Lambda^2},\ g^2 \gg g^2\frac{E^2}{\Lambda^2},\ g^3\frac{f_\pi}{E} \gg g^3\frac{Ef_\pi}{\Lambda^2} \gg g^4\frac{f_\pi^2}{\Lambda^2}\ . \tag{4.1}$$

In the TeV region, for $E \in (750\,\mathrm{GeV},\ 1.5\,\mathrm{TeV})$, this gives:

$$\begin{aligned}&(9.3, 37) \gg (0.55, 8.8), (2.0, 4.0) \gg (0.12, 0.93), (0.42, 0.42) \gg \\ &\quad (0.025, 0.099), (0.089, 0.045) \gg (5.3, 10.5)\times 10^{-3} \gg (1.1, 1.1)\times 10^{-3}\ ,\end{aligned} \tag{4.2}$$

where E is taken to be the invariant mass of the VV pair. The numerical values in (4.2) convincingly show the existence of the power counting hierarchy in (4.1). This determines the order of magnitude of all precise results from detailed calculations. This hierarchy makes it possible to classify the sensitivities of various scattering processes to the complete set of the effective operators in the EWCL. The construction of this power counting hierarchy can be understood as follows. The leading term $\frac{E^2}{f_\pi^2}$ in (4.1) comes from the model-independent lowest order $4V_L$ ($\neq 4Z_L$) scatterings. Starting from this leading term, (4.1) is built up by *increasing either the number of derivatives (i.e. the power of E/Λ) or the number of external transverse gauge bosons (i.e. the power of gauge coupling constants).* The next-to-leading-order contributions from the derivative expansion are always suppressed by E^2/Λ^2 relative to the model-independent leading term. Also, when each external V_L-line is replaced by the corresponding V_T-line, a factor $\frac{E}{f_\pi}$ in the amplitude would be replaced by a gauge coupling g (or g').[h] This explains why the power counting hierarchy takes the form of (4.1).

Table 3 is organized in accord with the power counting hierarchy given in (4.1) for VV scattering amplitudes. It shows the *relevant* effective new physics operators and the corresponding physical processes for probing the EWSB sector when calculating the scattering amplitudes to the required precision. For instance, the model-independent operator $\mathcal{L}_0$ can be probed via studying the leading tree-level scattering amplitude $T[4V_L]$ ($\neq T_0[4Z_L]$) which is of $O(\frac{E^2}{f_\pi^2})$. To test the model-dependent operators $\mathcal{L}_{4,5,6,7,10}$

[h] The counting on the amplitude $T[4W_T]$ is an exception of this rule because it can have a contribution from the vector-boson kinetic term. This exception can be found at the upper-right-hand corner of Table 1a.

demands a higher precision than the leading tree level contribution by a factor of $\frac{E^2}{\Lambda^2}$. For examples, in the high energy region, the $4V_L$ scatterings can sensitively probe $\mathcal{L}_{4,5}$, while $\mathcal{L}_{6,7}$ can be probed via $2W_L+2Z_L$ or $4Z_L$ scattering and $\mathcal{L}_{10}$ can only be tested via $4Z_L$ scattering. But, as shown in Table 3, to probe the operators $\mathcal{L}_{2,3,9,10,11;12}$, one has to detect the $3V_L + V_T$ scatterings, which are further suppressed by a factor $\frac{M_W}{E}$ relative to the leading model-dependent contributions from the $\mathcal{L}_{4,5}$ and $\mathcal{L}_{6,7,10}$ via $4V_L$ processes. Since the model-independent leading order $2V_T+2V_L$ and $4V_T$ amplitudes (from $\mathcal{L}_0$) and the largest constant B-term ($B_0^{(0)}$) are all of the same order, i.e. $O(g\frac{E}{f_\pi}\frac{E^2}{\Lambda^2}, g^2)$ [cf. (4.2)],[i] it requires a significantly higher precision to sensitively probe these operators which can only contribute the g-suppressed indirect EWSB information and therefore are more difficult to be tested. Finally, the operators $\mathcal{L}_{1,8;13,14}$ can be probed via the amplitude $T_1[2V_L, 2V_T]$ ($\neq T_1[2Z_L, 2Z_T]$) which is of $O(g^2\frac{E^2}{\Lambda^2}, g^3\frac{f_\pi}{E})$ and numerically much smaller [cf. (4.2)]. Therefore, $\mathcal{L}_{1,8;13,14}$ should be effectively probed via scattering processes other than the VV-fusion, for instance, via $q\bar{q} \to VV$.

In summary, applying the power counting technique allows us to conveniently estimate contributions of various operators to any scattering amplitude. For a given scattering process, this result tells us which operators can be sensitively probed. Similarly, the same result can also tells us which process would be most sensitive for probing new physics via a given effective operator. In the next section, we shall examine the $W^+W^+ \to W^+W^+$ process at the LHC to illustrate how to use the electroweak power counting method to estimate the event rates and how to use the ET as a physical criterion to classify the sensitivity of this scattering process to the next-to-leading order bosonic operators in the EWCL.

5. Probing EWSB Mechanism at the LHC via Weak-Boson Scatterings

In this section, we shall study the production rate of $W^+W^+ \to W^+W^+$ at the LHC. To calculate the event rate, we multiply the luminosity of the incoming weak-boson pair VV (obtained by using the effective-W approximation [16]) and the constituent

[i] They can in principle be separated if the polarization of the external V-lines are identified. For the final state V's, one can study the angular distribution of the leptons from V-decay. For the incoming V's, one can use forward-jet tagging and central-jet vetoing to select longitudinal V's [15].

cross section of the weak-boson scattering (derived from the amplitude which has been estimated by our power counting analysis in the last section). Note that the validity of the effective-W approximation requires the VV invariant mass $M_{VV} \gg 2M_W$ [16], which coincides with the condition in (2.3a) for ignoring the LNI B-term to apply the ET.[j] Thus, the effective-W approximation and the ET have similar precisions in computing the event rate from $V_L V_L$ fusion process in hadron collisions. As M_{VV} increases, they become more accurate. It is known that the effective-W approximation is less accurate for sub-processes involving transverse gauge bosons. Generally speaking, a factor of 2 to 5 uncertainty in its rate is understood [17]. Nevertheless, the effective-W method has been widely used in the literature for calculating event rates from gauge-boson (either transversely or longitudinally polarized) fusion processes because it is easy to implement and can be used to reasonably estimate event rates before any exact calculation is available. As to be shown shortly, our power counting analysis for the constituent cross section agrees well with explicit calculation within a factor of 2. Hence, it is appropriate to apply the power counting analysis together with the effective-W approximation for estimating the event rates from weak-boson fusion at the LHC. When applying our power counting analysis, we have reasonably ignored the angular dependence in the scattering amplitudes (cf. Tables 1$\sim$2) because it will not affect the order of magnitude estimates for the total cross sections (or the event rates).

Let us denote the production rate for the scattering process $W^+_\alpha W^+_\beta \to W^+_\gamma W^+_\delta$ as $R_{\alpha\beta\gamma\delta(\ell)}$, where $\alpha, \beta, \gamma, \delta = L, T$ label the polarizations of the W-bosons and $\ell = 0, 1, \cdots$ indicates contributions from tree, 1-loop, $\cdots$, respectively. Up to the one-loop level, we define

$$\begin{aligned} R_{\alpha\beta\gamma\delta} &= R_{\alpha\beta\gamma\delta(0)} + R_{\alpha\beta\gamma\delta(1)} \quad , \\ R_{\alpha\beta\gamma\delta(\pm)} &= R_{\alpha\beta\gamma\delta(0)} \pm |R_{\alpha\beta\gamma\delta(1)}| \quad . \end{aligned} \tag{5.1a, b}$$

Also, we use R_B to denote the rate contributed by the largest B-term in the $VV \to VV$ scatterings, which is $O(g^2)$, cf. (2.5). For convenience, we use the subscript "$_S$" to stand for summing up the polarizations of the corresponding gauge boson.

To check the reliability of our power counting method, we have compared our results for the W^+W^+ scatterings with those in Fig. 8 of Ref. [18] in which all the initial

[j] Here, we have reasonably taken the typical energy scale E of the VV scattering to be M_{VV} to estimate the event rates.

state polarizations of the weak-bosons were summed over.[k] As shown in Fig. 1, both results coincide well within a factor of 2. This is a convincing example showing that the semi-quantitative physical picture can be quickly grasped by our power counting analysis without performing complicated precise numerical calculations.

In Fig. 2a we give our power counting estimates for the LHC production rates of the $W_L^+W_L^+$ pairs from different polarizations of the initial state W-bosons. In this plot, we did not include any finite part of contributions from the next-to-leading-order operators by setting the renormalized coefficients $\ell_{0\sim 14}$ to be zero.[l] As clearly shown in Fig. 2a, the rate from $4W_L$ scattering dominates and the rate from $W_T + 3W_L$ scattering is lower by about an order of magnitude for large M_{WW} in spite of the fact that the W_TW_L luminosity is larger than the W_LW_L luminosity in the initial state. Also separately shown in the same figure is the event rate $|R_B|$ contributed by the largest B-term [cf. (2.1) and (2.5)] which is even significantly lower than that from the $W_T + 3W_L$ scattering by a factor of $2 \sim 7$ for $M_{WW} > 500\,\mathrm{GeV}$. However, the rate from W_TW_T initial state is lower than that from the B-term in the $4W_L$ amplitude as $E \geq 600\,\mathrm{GeV}$. This implies that if the contribution from W_TW_T initial state is to be included in calculating the total production rate of the W_LW_L pair, the contribution from the B-term in the $4W_L$ amplitude also has to be included because they are of the same order in magnitude. If, however, only the pure Goldstone boson amplitude $T[\pi^+\pi^+ \to \pi^+\pi^+]$ is used to calculate the $4W_L$-amplitude (with the B-term ignored) the contribution from $T[W_T^+W_T^+ \to W_L^+W_L^+]$ should also be consistently ignored for computing the total rate of $W_L^+W_L^+$ pair production via the weak-boson fusion mechanism.

As shown in Ref. [14], it is possible to statistically, though not on the event-by-event basis, choose event with longitudinally polarized W-bosons in the initial state by applying the techniques of forward-jet tagging and central-jet vetoing. In this work we do not intend to study the details of the event kinematics, and we shall sum over all the initial state polarizations for the rest of discussions. Let us first compare the rates for different polarizations in the final state. Fig. 2b shows that the rate of W_LW_L final state

[k] We have adopted the same effective-W approximation as Ref. [18].

[l] It is understood that the divergent pieces from one-loop calculations have been absorbed by the coefficients of the corresponding next-to-leading-order effective operators [10, 12].

dominates, while the rate of B-term and the rates of W_LW_T and W_TW_T final states are of the same order, and all of them are about an $O(10)$ to $O(10^2)$ lower than the rate of W_LW_L final state in the energy region $E = M_{WW} > 500\,\text{GeV}$. This makes it clear that if one wants to increase the precision in calculating the total event rates by including the small contribution from the B-term in pure $4W_L^+$ scattering, then the contributions from $W_S^+W_S^+ \to W_T^+W_T^+$ and $W_S^+W_S^+ \to W_L^+W_T^+$ scatterings should also be consistently included. Otherwise, they must all be neglected together. Hence, from Figs. 2a and 2b, we conclude that the scattering process $W_L^+W_L^+ \to W_L^+W_L^+$ dominates the W^+W^+-pair productions when all the model-dependent coefficients $\ell_{0\sim14}$ in (3.6) are set to be zero.

For nonvanishing $\ell_{0\sim14}$, we classify the sensitivities to all the next-to-leading-order bosonic operators at the LHC via the scattering process $W^+W^+ \to W^+W^+$. Our criterion for discriminating different sensitivity levels (sensitive, marginally sensitive, or insensitive) to probe a particular operator via the production of W^+W^+ pairs is to compare its contribution to the event rate ($|R_{\alpha\beta\gamma\delta(1)}|$) with that from the largest model-independent contribution of the LNI B-term ($|R_B|$). Without knowing the values of the *model-dependent coefficients* (ℓ_i's), we show in Figs. 3$\sim$4 the results for varying $|\ell_i|$ from $O(1)$ to $O(10)$. Here, the polarizations of the initial and the final states have been summed over. In Figs. 3a and 3b, we consider the coefficients (ℓ_i's) to be naturally of $O(1)$ according to the naive dimensional analysis [12]. Fig. 3a shows that the event rates/$(100\,\text{fb}^{-1}$ GeV) from operators $\mathcal{L}_{4,5}$ are larger than that from the B-term when $E = M_{WW} > 600$ GeV, while the rates from operators $\mathcal{L}_{3,9,11;12}$ can exceed $|R_B|$ only if $E = M_{WW} > 860$ GeV. As M_{WW} increases, the rates contributed by $\mathcal{L}_{4,5}$ remain flat, while the rates by $\mathcal{L}_{3,9,11;12}$ and the B-term decrease. The ratio of the event rates from $\mathcal{L}_{4,5}$ to $|R_B|$ is 5.0 at $E = M_{WW} = 1\,\text{TeV}$, and rapidly increases to 19.6 at $E = M_{WW} = 1.5$ TeV. In contrast, the ratio between the rates from $\mathcal{L}_{3,9,11;12}$ and the B-term only varies from 1.4 to 3.0 for $E = M_{WW} = 1 \sim 1.5\,\text{TeV}$, which means that they are of the same order. Fig. 3b shows that for the coefficients of $O(1)$, the event rates contributed by operators $\mathcal{L}^{(2)\prime}$ and $\mathcal{L}_{1,2,8;13,14}$ are all below $|R_B|$ for a wide region of energy up to about $2\,\text{TeV}$, so that they cannot be sensitively probed in this case. Especially, the contributions from $\mathcal{L}_{1,13}$ are about two orders of magnitude lower than that from the B-term. This suggests that $\mathcal{L}_{1,13}$ must be tested via other processes.

In Figs. 4a and 4b, different event rates are compared for the coefficients (ℓ_i's) to be of $O(10)$. Fig. 4a shows that the rates from $\mathcal{L}_{3,9,11;12}$ could significantly dominate $|R_B|$ by an order of magnitude for $E = M_{WW} \sim 1\,\text{TeV}$ if their coefficients are increased by a factor of 10 relative to the natural size of $O(1)$. Fig. 4b shows that the rates from $\mathcal{L}_{1,13}$ is still lower than $|R_B|$ by about an order of magnitude, while the rate from $\mathcal{L}_2$ is close to $|R_B|$ within a factor of 2. The contributions from $\mathcal{L}_{8;14}$ and $\mathcal{L}^{(2)\prime}$ exceed $|R_B|$ by about a factor $2 \sim 3$ at $E = M_{WW} = 1\,\text{TeV}$ and a factor $3 \sim 5$ at $E = M_{WW} = 1.5\,\text{TeV}$ when their coefficients are of $O(10)$.

From the above analyses, we conclude that studying the $W^+W^+ \to W^+W^+$ process can sensitively probe the operators $\mathcal{L}_{4,5}$, but is only marginally sensitive for probing $\mathcal{L}_{3,9,11;12}$ and insensitive for $\mathcal{L}^{(2)\prime}$ and $\mathcal{L}_{1,2,8;13,14}$, if their coefficients are naturally of $O(1)$. In the extreme case where their coefficients are of $O(10)$, the probe of $\mathcal{L}_{3,9,11;12}$ could become sensitive and that of $\mathcal{L}^{(2)\prime}$ and $\mathcal{L}_{8;14}$ could become marginally sensitive, while $\mathcal{L}_2$ and $\mathcal{L}_{1;13}$ still cannot be sensitively measured.

Finally, we note that the operators $\mathcal{L}_{6,7,10}$, which violate the custodial $SU(2)_C$ symmetry, do not contribute to the W^+W^+ pair productions up to the one-loop order. They can however contribute to the other scattering channels such as $WZ \to WZ$, $WW \to ZZ$, $ZZ \to WW$ and $ZZ \to ZZ$, cf. Table 3.[m] By our order of magnitude estimates, we conclude that they will give the similar kind of contributions to the WZ or ZZ channel as $\mathcal{L}_{4,5}$ give to the W^+W^+ channel. This is because all these operators contain four covariant derivatives [cf. (3.6)].

Before concluding this section, we would like to comment on the $W^-W^- \to W^-W^-$ production process. At the LHC (a pp collider), in the TeV region, the luminosity of W^-W^- is typically smaller than that of W^+W^+ by a factor of $3 \sim 5$. This is because in the TeV region, where the fraction of momentum (x) of proton carried by the quark which emitting the initial state W-boson is large (for $x = \frac{E}{\sqrt{S}} \sim 0.1$), the parton luminosity is dominated by the valence quark contributions. Since in the large-x region, the probability of finding a down-type valence quark in the proton is smaller than finding an up-type valence quark, the luminosity of W^-W^- is smaller than that of W^+W^+. However, as long as there are enough W^-W^- pairs detected, which requires a large integrated luminosity of

[m] $\mathcal{L}_{10}$ only contributes to $ZZ \to ZZ$ channel.

the machine and a high detection efficiency of the detector, a similar conclusion on probing the effective operators for the W^+W^+ channel can also be drawn for this channel. For $M_{WW} > 1.5\,\text{TeV}$, the W^-W^- production rate becomes about an order of magnitude smaller than the W^+W^+ rate for any given operator. Thus, this process could not be sensitive to all these operators in this very high energy region.

6. Conclusions

In this work, based upon our recent study on the intrinsic connection between the longitudinal weak-boson scatterings and probing the EWSB sector, we first formulate the physical content of the ET as a criterion for discriminating physical processes which are sensitive/insensitive to probing the EWSB mechanism [cf. Eqs. (2.3)$\sim$(2.5)]. Then, we develop a precise power counting rule (3.7) for the EWCL, from a natural generalization of Weinberg's counting method for low energy QCD interaction.

Armed with this powerful counting rule and using the ET as the physical criterion for probing the EWSB sector, we further systematically classify the sensitivities of various scattering processes to the complete set of bosonic operators at the level of S-matrix elements (cf. Tables 1$\sim$3). The power counting hierarchy in (4.1) governs the order of magnitude of all relevant scattering amplitudes.

In the EWCL formalism, the leading contribution from the LNI B-term is found to be model-independent and contains only the SM gauge coupling constant [cf. (2.5) and Fig. 5c in the Appendix]. All other parts in the B-terms are further suppressed by a factor $\frac{M_W}{E}$ or $\left(\frac{(E,\, gf_\pi)}{\Lambda}\right)^2$ relative to the leading contribution given in (2.5), cf. Table 2. Thus, they are negligibly small and insensitive to probing the EWSB sector. It is important to note that the model-independent leading B-term (2.5) provides a very useful criterion for discriminating among sensitive, marginally sensitive, and insensitive contributions from the various new physics effective operators in (3.6).

Finally, based on the above power counting analysis combined with the effective-W approximation, we phenomenologically probe the EWSB sector at the LHC via the weak-boson scattering in the same-charged channel: $W^\pm W^\pm \to W^\pm W^\pm$. Computed from this simple power counting analysis, our numerical results for the LHC production rates

coincide with those explicit calculations performed in the literature well within a factor of 2 (cf. Fig. 1). This indicates that our power counting analysis can provide an elegant grasp of the overall semi-quantitative physical picture. We perform the first complete, semi-quantitative survey on the sensitivities of all fifteen next-to-leading-order CP-conserving and CP-violating effective operators at the LHC via the W^+W^+ channel. The results are shown in Figs. 3$\sim$4. We find that, for this channel, when the coefficients ℓ_n's are naturally of $O(1)$, $\mathcal{L}_{4,5}$ are most sensitive, $\mathcal{L}_{3,9,11;12}$ are marginally sensitive, and $\mathcal{L}^{(2)\prime}$ and $\mathcal{L}_{1,2,8;13,14}$ are insensitive. For the extreme case where the coefficients are of $O(10)$, then the probe of $\mathcal{L}_{3,9,11;12}$ could become sensitive and that of $\mathcal{L}^{(2)\prime}$ and $\mathcal{L}_{8;14}$ could become marginally sensitive, while $\mathcal{L}_2$ and $\mathcal{L}_{1;13}$ still cannot be sensitively measured via this process so that they must be measured via other processes (*e.g.*, $q\bar{q} \to VV$). Up to the next-to-leading order, the $SU(2)_C$-violating operators $\mathcal{L}_{6,7,10}$ do not contribute to this process. They, however, can be probed via the WZ and ZZ productions.

A similar conclusion holds for the W^-W^- channel except that the event rate is lower by about a factor of $3 \sim 5$ in the TeV region because the quark luminosity for producing a W^-W^- pair is smaller than that for a W^+W^+ pair in pp collisions.

Acknowledgements We thank Sally Dawson for discussion on the effective-W approximation used in Ref. [18], and William A. Bardeen for useful suggestion. H.J.H. is supported in part by the U.S. DOE under grant DEFG0592ER40709; Y.P.K. is supported by the NSF of China and the FRF of Tsinghua University; C.P.Y. is supported in part by the NSF under grant PHY-9309902.

Appendix: Validity of the ET in some special kinematic regions

Here we examine the validity of the ET in some special kinematic regions and its physical implication in probing the EWSB, which often cause confusion in the literature. It is known that there are kinematic regions in which the Mandelstam variables t or u is small or even vanishing despite the fact that $\sqrt{s} \gg M_W$ for high energy scatterings. Therefore, the amplitude that contains a t- or u-channel diagram with massless photon

field can generate a kinematic singularity when the scattering angle θ approaches to 0 or π. In the following, we study in such special kinematic regions whether the B-term [cf. (2.1)] can be safely ignored to validate the ET and its physical consequence to probing the EWSB sector.

For illustration, let us consider the tree level $W_L^+W_L^- \to W_L^+W_L^-$ scattering in the chiral Lagrangian formalism. Generalization to loop orders is obvious since the kinematic problem analyzed here only concerns the one-particle-reducible (1PR) internal W, Z or photon line in the t-channel (or u-channel) diagram. Both the tree level $W_L^+W_L^- \to W_L^+W_L^-$ and $\pi^+\pi^- \to \pi^+\pi^-$ amplitudes in the chiral Lagrangian formalism contain contact diagrams, s-channel Z-exchange and photon-exchange diagrams, and t-channel Z-exchange and photon-exchange diagrams. In the C.M. frame, the two tree-level amplitudes $T[W_L]$ and $T[\mathrm{GB}]$ are precisely:

$$T[W_L] = ig^2\left[-(1+\kappa)^2\sin^2\theta + 2\kappa(1+\kappa)(3\cos\theta-1) - \mathrm{c_w^2}\frac{4\kappa(2\kappa+3)^2\cos\theta}{4\kappa+3-\mathrm{s_w^2c_w^{-2}}}\right.$$
$$\left.+\mathrm{c_w^2}\frac{8\kappa(1+\kappa)(1-\cos\theta)(1+3\cos\theta)+2[(3+\cos\theta)\kappa+2][(1-\cos\theta)\kappa-\cos\theta]^2}{2\kappa(1-\cos\theta)+\mathrm{c_w^{-2}}}\right]$$
$$+ie^2\left[-\frac{\kappa(2\kappa+3)^2\cos\theta}{\kappa+1}+4(1+\kappa)(1+3\cos\theta)+\frac{[(3+\cos\theta)\kappa+2][(1-\cos\theta)\kappa-\cos\theta]^2}{\kappa(1-\cos\theta)}\right] \quad , \tag{A1a}$$

$$T[\mathrm{GB}] = ig^2\left[\frac{(1+\cos\theta)}{2}\kappa+\frac{1}{3}+\frac{(\mathrm{c_w^2}-\mathrm{s_w^2})^2}{2\mathrm{c_w^2}}\left(-\frac{2\kappa\cos\theta}{4\kappa+3-\mathrm{s_w^2c_w^{-2}}}+\frac{(3+\cos\theta)\kappa+2}{2(1-\cos\theta)\kappa+\mathrm{c_w^{-2}}}\right)\right]$$
$$+ie^2\left[-\frac{4\kappa\cos\theta}{4\kappa+1}+\frac{(3+\cos\theta)\kappa+2}{(1-\cos\theta)\kappa}\right] \quad , \tag{A1b}$$

where $\kappa \equiv p^2/M_W^2$ with p equal to the C.M. momentum; $\mathrm{s_w} \equiv \sin\theta_\mathrm{W}$, $\mathrm{c_w} \equiv \cos\theta_\mathrm{W}$ with θ_W equal to the weak mixing angle; and θ is the scattering angle. In (A1a) and (A1b) the terms without a momentum factor in the denominator come from contact diagrams, terms with denominator independent of scattering angle come from s-channel diagrams and terms with denominator containing a factor $1-\cos\theta$ are contributed by t-channel diagrams. Let us consider two special kinematic regions defined below.

(i). In the limit of $\theta \to 0$:

As $\theta \to 0$, the t-channel photon propagator has a kinematic pole, but both W_L and GB amplitudes have the *same* pole structure, i.e.

$$(T[W_L]-T[\mathrm{GB}])_{\text{pole term}} = ie^2(2\kappa^{-1}+3+\cos\theta)[(1-\cos\theta)\kappa^2-2\kappa\cos\theta-(1+\cos\theta)] \ , \quad (A2)$$

which is finite.[n] Hence, *the B-term, which is defined as the difference* $T[W_L]-T[\mathrm{GB}]$ *, is finite at* $\theta = 0$ *, and is of* $O(e^2)$ *which is smaller than* $O(g^2)$. This means that when θ is close to the t-channel photon pole, the B-term is negligibly small relative to the GB-amplitude so that (2.3b) is satisfied and the ET works. More explicitly, in the limit of $\theta = 0$ (i.e. $t = 0$), and from (A1a,b), the W_L and GB amplitudes are

$$\begin{aligned} T[W_L] &= i\left[4(3-8\mathrm{c_w^2}+8\mathrm{c_w^4})\frac{p^2}{f_\pi^2}+2e^2\left(2+\frac{M_W^2}{p^2}\right)\frac{1}{1-c_0}\right]+O(g^2) \ , \\ T[\mathrm{GB}] &= i\left[4(3-8\mathrm{c_w^2}+8\mathrm{c_w^4})\frac{p^2}{f_\pi^2}+2e^2\left(2+\frac{M_W^2}{p^2}\right)\frac{1}{1-c_0}\right]+O(g^2) \ , \\ T[W_L] &= T[\mathrm{GB}]+O(g^2) \ , \end{aligned} \quad (A3)$$

where $c_0 \equiv \lim_{\theta\to 0}\cos\theta$. In this case one cannot make the M_W^2/t expansion[o] because t vanishes identically. Since both W_L and GB amplitudes have exactly the same kinematic singularity and the B-term is much smaller than $T[\mathrm{GB}]$, *the ET still holds* in this special kinematic region. We also emphasize that *in the kinematic regions where* t *or* u *is not much larger than* M_W^2*, the* t*-channel or* u*-channel internal gauge boson lines must be included according to the precise formulation of the ET* [cf. (2.3) and (2.3a,b)].[p]

(ii). In the limit of $\theta \to \pi$:

In this kinematic region, $s,\ t \gg M_W^2$, and (A1a,b) yield

$$\begin{aligned} T[W_L] &= i\left[2(1+\cos\theta)\frac{p^2}{f_\pi^2}+O(g^2)\right] \ , \\ T[\mathrm{GB}] &= i\left[2(1+\cos\theta)\frac{p^2}{f_\pi^2}+O(g^2)\right] \ , \\ T[W_L] &= T[\mathrm{GB}]+O(g^2) \ , \end{aligned} \quad (A4)$$

[n] This conclusion can be directly generalized to other t- or u-channel processes.

[o] This expansion is *unnecessary* for the validity of the ET, cf. (2.3) and (2.3a,b).

[p] This does not imply, in any sense, a violation of the ET since the ET, cf. (2.3) and (2.3a,b), does not require either $t \gg M_W$ or $u \gg M_W$.

where the $O(g^2)$ term is the largest term we ignored which denotes the order of the B-term [cf. (2.5)]; all other terms we ignored such as $O(M_W^2/p^2)$ or $O(e^2)$ are smaller than $O(g^2)$ and thus will not affect the order of magnitude estimate of the B-term. For $s,\ t \gg M_W^2$, the W_L and GB amplitudes are dominated by the p^2-term in (A4), which is actually proportional to u for this process. When the scattering angle θ is close to 180°, u becomes small and thus this leading p^2 term is largely suppressed so that both the W_L and GB amplitudes can be as small as the B-term, i.e. of $O(g^2)$. In this case our condition (2.3a) is satisfied while (2.3b) is not, which means that the EWSB sector cannot be sensitively probed for this kinematic region. Since the total cross section of this process is not dominated by this special kinematic region and is mainly determined by the un-suppressed leading large p^2-term, so *the kinematic dependence of the amplitude will not affect the order of magnitude of the total cross section.* Hence, *our application of the power counting analysis in Sec. 5 for computing the total event rates remains valid even though we have ignored the angular dependence in estimating the magnitude of the scattering amplitudes.* Neglecting the angular dependence in the amplitude may cause a small difference in the event rate as compared to that from detailed precise calculations. For the processes such as $W_L^\pm W_L^\pm \to W_L^\pm W_L^\pm$ and $W_L^+ W_L^- \to Z_L Z_L$, the leading p^2-term is proportional to s/f_π^2 with no angular dependence, so that the angular integration causes *no difference* between our power counting analysis and the exact calculation for the leading p^2-term contribution.[q] In the above example for $W_L^+ W_L^- \to W_L^+ W_L^-$ channel [cf. (A4)], the leading amplitude is proportional to $-u/f_\pi^2$. Using the power counting method, we ignore the θ-dependence and estimate it as s/f_π^2 . In computing the total rate, we integrate out the scattering angle. This generates a difference from the precise one:

$$\frac{\int_{-1}^{1} u^2 \, \mathrm{d}\cos\theta}{\int_{-1}^{1} s^2 \, \mathrm{d}\cos\theta} = \frac{1}{3} \quad ,$$

which, as expected, is only a factor of 3 and does not affect our order of magnitude estimates.

Finally, we make a precise numerical analysis on the equivalence between the W_L and GB amplitudes to show how well the ET works in different kinematic regions and its

[q] The small difference (a factor of 1.4) in Fig. 1 mainly comes from neglecting the tree level sub-leading terms in our order of magnitude estimate for the amplitudes.

implication to probing the EWSB sector. We use the full expressions (A1a,b) for W_L and GB amplitudes as required by the ET, cf. (2.3) and (2.3a,b). In Fig. 5a, we plot the ratio $|B/g^2|$ for scattering angle $\theta = 2°, 10°, 45°, 90°, 100°, 120°, 135°, 150°, 180°$. Fig. 5a shows that the LNI B-term is *always of* $O(g^2)$ *in the whole kinematic region,* and thus is irrelevant to the EWSB sector, in accord with our general physical analysis in Sec. 2. Hence, to have a sensitive probe of the EWSB mechanism, condition (2.3b) or (2.4) must be satisfied. Fig. 5b shows that for $0 \leq \theta \leq 100°$, the ratio $|B/T[W_L]| \leq 10\%$ when $M_{WW} \geq 500\,\text{GeV}$. For $\theta \geq 120°$, this ratio becomes large and reaches $O(1)$ when θ is close to 180°. This is because the kinematic factor $(1 + \cos\theta)$, associated with the leading p^2 term [cf. (A4)], becomes small. This, however, will not alter the conclusion that for $4W_L$-scattering the total cross section from T[GB] is much larger than that from the B-term as $M_{WW} \geq 500\,\text{GeV}$. Note that in Fig. 5b, for $\theta \leq 10°$, i.e. close to the t-channel photon pole, the ratio $|B/T[W_L]|$ is below 1% and thus the ET holds very well. In Fig. 5c, we plot both the W_L and GB amplitudes for $\theta = 10°, 45°, 100°, 150°$. The solid lines denote the complete W_L amplitude and the other lines denote the GB amplitude. We find that when $\theta \leq 100°$, the GB amplitude is almost indistinguishable from the W_L amplitude. For $\theta = 150°$, the W_L amplitude is of the same order as the B-term, i.e. of $O(g^2)$, when $M_{WW} < 1\,\text{TeV}$. In this case the W_L or GB amplitude is too small and the strongly coupled EWSB sector cannot be sensitively probed. As the energy E increases, we see that the W_L and GB amplitudes rapidly dominate over the B-term and agree better and better even for large scattering angles.

The above conclusions hold for the tree level contributions from the lowest order operators in $\mathcal{L}_G + \mathcal{L}^{(2)} + \mathcal{L}_F$, cf. (3.6). However, independent of the kinematic region considered, not all the contributions from the next-to-leading-order effective operators can dominate the B-term and satisfy the condition (2.3b). This is why the condition (2.3b) can serve as the criterion for classifying the sensitivities of these next-to-leading-order operators in probing the EWSB sector for each given process.

We conclude that *the B-term as defined in (2.1) can be at most of* $O(g^2)$ *for all kinematic regions* (cf. Fig. 5a), and is insensitive to the EWSB mechanism, in accord with our general analysis in Sec. 2. *When* t *or* u *is not large, the* t*- or* u*-channel internal lines must be included.* We find that *even for* t *or* u *being close to zero, the ET*

still works well [cf. Eq. (A3) and Fig. 5b]. This is because the validity of the ET does not require either $t \gg M_W^2$ or $u \gg M_W^2$, cf. (2.3) and (2.3a,b). For some scattering processes, there may be special kinematic regions in which the GB and W_L amplitudes are largely suppressed[r] so that the EWSB sector cannot be sensitively probed in these special kinematic regions. However, it can still be sensitively probed by measuring the total event rates from these processes.

[r] This large suppression can also arise from the polarization effects of the in/out states.

References

1. M. Veltman, Acta. Phys. Pol. **B8** (1977) 475;
   M.B. Einhorn and J. Wudka, Phys. Rev. **D39** (1989) 2758; *ibid*, **D47** (1993) 5029.
2. For a recent systematical investigation on this LNI ambiguity, see:
   H.-J. He, Y.-P. Kuang, C.-P. Yuan, Phys. Rev. **D51** (1995) 6463.
3. J.M. Cornwall, D.N. Levin, and G. Tiktopoulos, Phys. Rev. **D10** (1974) 1145;
   C.E. Vayonakis, Lett. Nuovo. Cimento **17** (1976) 383;
   B.W. Lee, C. Quigg, and H. Thacker, Phys. Rev. **D16** (1977) 1519;
   M.S. Chanowitz and M.K. Gaillard, Nucl. Phys. **B261** (1985) 379;
   G.J. Gounaris, R. Kögerler, and H. Neufeld, Phys. Rev. **D34** (1986) 3257;
   H. Veltman, *ibid*, **D41** (1990) 2294.
4. Y.-P. Yao and C.-P. Yuan, Phys. Rev. **D38** (1988) 2237;
   J. Bagger and C. Schmidt, Phys. Rev. **D41** (1990) 264;
   H.-J. He, Y.-P. Kuang, and X. Li, Phys. Rev. Lett. **69** (1992) 2619;
   Phys. Rev. **D49** (1994) 4842; Phys. Lett. **B329** (1994) 278;
   A. Dobado and J.R. Pelaez, Phys. Lett. **B329** (1994) 469 (Addendum, ibid, **B335**, 554); Nucl. Phys. **B425**(1994)110, (Errata, *ibid*, **B434** (1995) 475).
5. H.-J. He, Y.-P. Kuang and X. Li, in Ref. [4];
   H.-J. He, Y.-P. Kuang and C.-P. Yuan, in Ref. [2].
6. See, *e.g.*, C. Grosse-Knetter and I. Kuss, BI-TP/10; D. Espriu and J. Matias, UB-ECM-PF-94/16.
7. S. Weinberg, Physica **96A** (1979) 327.
8. H.-J. He, Y.-P. Kuang, C.-P. Yuan, VPI-IHEP-95-09 (in preparation).
9. See, *e.g.*, H. Veltman, in Ref. [3].
10. T. Appelquist and C. Bernard, Phys. Rev. **D22** (1980) 200;
    A.C. Loghitano, Nucl. Phys. **B188** (1981) 118;
    T. Appelquist and G.-H. Wu, Phys. Rev. **D48** (1993) 3235; and references therein.
11. R.D. Peccei and X. Zhang, Nucl. Phys. **B337** (1990) 269;
    E. Malkawi and C.-P. Yuan, Phys. Rev. **D50** (1994) 4462.
12. H. Georgi, *Weak Interaction and Modern Particle Theory*, Benjamin/Cummings Publishing Company, 1984;

A. Manohar and H. Georgi, Nucl. Phys. **B234** (1984) 189.

13. For recent reviews, F. Feruglio, Inter. J. Mod. Phys. **A8** (1993) 4937; J. Wudka, *ibid*, **A9** (1994) 2301.
14. J. Bagger, V. Barger, K. Cheung, J. Gunion, T. Han, G.A. Ladinsky, R. Rosenfeld and C.–P. Yuan, Phys. Rev. **D49** (1994) 1; and preprint MSUHEP-50305, Phys. Rev. **D** (1995) (to be published).
15. C.–P. Yuan, published in "Perspectives on Higgs Physics", edited by Gordon L. Kane, World Scientific, 1992.
16. J.F. Gunion, H.E. Haber, G.L. Kane and S. Dawson, *The Higgs Hunter's Guide*, (Addison-Wesley Pub. Company, 1990);
    S. Dawson, Nucl. Phys. **B249** (1985) 42; and references therein.
17. J.F. Gunion, J. Kalinowksi, and A. Tofighi-Niaki, Phys. Rev. Lett. **57** (1986) 2351.
18. J. Bagger, S. Dawson and G. Valencia, Nucl. Phys. **B399** (1993) 364.

Table Captions

Table 1. Estimates of amplitudes for $W^{\pm}W^{\pm} \to W^{\pm}W^{\pm}$ scattering.

Table 1a. Model-independent contributions from $\mathcal{L}_G + \mathcal{L}_F + \mathcal{L}^{(2)}$.

Table 1b. Model-dependent contributions from the next-to-leading-order effective operators.

Table 2. Order estimates of B-terms for $W^{\pm}W^{\pm} \to W^{\pm}W^{\pm}$ scattering.

Table 2a. Model-independent contributions.

Table 2b. Relevant operators for model-dependent contributions.[(a)]

Notes:

[(a)] We list the relevant operators for each order of B-terms.

[(b)] Here $B_1^{(0)}$ is contributed by $T_1[2\pi^{\pm}, 2v^{\pm}]$.

Table 3. Global classification of sensitivities to probing direct and indirect EWSB information from effective operators at the level of S-matrix elements.[(a)]

Notes:

[(a)] The contributions from $\mathcal{L}_{1,2,13}$ are *always* associated with a factor of $\sin^2\theta_W$, unless specified otherwise.

[(b)] MI = model-independent, MD = model-dependent.

[(c)] There is no contribution when all the external lines are electrically neutral.

[(d)] $B_0^{(1)} \simeq T_0[2\pi, v, V_T]$ $(\neq T_0[2\pi^0, v^0, Z_T])$, $B_0^{(3)} \simeq T_0[v, 3V_T]$ $(\neq T_0[v^0, 3Z_T])$.

[(e)] $T_1[2V_L, 2V_T] = T_1[2Z_L, 2W_T]$, $T_1[2W_L, 2Z_T]$, or $T_1[Z_L, W_L, Z_T, W_T]$.

[(f)] $\mathcal{L}_2$ only contributes to $T_1[2\pi^{\pm}, \pi^0, v^0]$ and $T_1[2\pi^0, \pi^{\pm}, v^{\pm}]$ at this order; $\mathcal{L}_{6,7}$ do not contribute to $T_1[3\pi^{\pm}, v^{\pm}]$.

[(g)] $\mathcal{L}_{10}$ contributes only to $T_1[\cdots]$ with all the external lines being electrically neutral.

[(h)] Here, $T_1[2W_L, 2W_T]$ contains a coupling $e^4 = g^4 \sin^4\theta_W$.

[(i)] $\mathcal{L}_2$ only contributes to $T_1[3\pi^{\pm}, v^{\pm}]$.

[(j)] $\mathcal{L}_{1,13}$ do not contribute to $T_1[2\pi^{\pm}, 2v^{\pm}]$.

Figure Captions

Fig. 1. Comparison with the Fig. 8 of Ref. [18] up to 1-loop for $\sqrt{S} = 40\,\text{TeV}$. The solid and long-dashed lines are given by our power counting analysis. The dashed and dot-dashed lines are R_{LLLL} and R_{TTLL} of Ref. [18] which coincide with ours within a factor of 2. [The meanings of the production rates $R_{\alpha\beta\gamma\delta}$'s are defined in the text, cf. (5.1a,b).]

Fig. 2.
(2a). Comparison of the production rates of $W_L^+W_L^+$ pairs up to 1-loop for the $W_L^+W_L^+$, $W_L^+W_T^+$ and $W_T^+W_T^+$ initial states, at the 14 TeV LHC.
(2b). Comparison of the production rates of different final states up to 1-loop after summing over the polarizations of the initial states, at the 14 TeV LHC.

Fig. 3. Sensitivities of operators $\mathcal{L}^{(2)\prime}$ and $\mathcal{L}_{1\sim14}$, when their coefficients are of $O(1)$, at the 14 TeV LHC.

(3a). For operators $\mathcal{L}_{4,5,3,9,11,12}$.
(3b). For operators $\mathcal{L}^{(2)\prime}$ and $\mathcal{L}_{1,2,8,13,14}$.

Fig. 4. Same as Fig. 3, but the coefficients ℓ_n's are of $O(10)$.

(4a). For operators $\mathcal{L}_{4,5,3,9,11,12}$.
(4b). For operators $\mathcal{L}^{(2)\prime}$ and $\mathcal{L}_{1,2,8,13,14}$.

Fig. 5. Examination on the kinematic dependence and the validity of the ET for the $W_L^+W_L^- \to W_L^+W_L^-$ scattering process.

(5a). The ratio $|B/g^2|$ for $\theta = 2^\circ,\ 10^\circ,\ 45^\circ,\ 90^\circ,\ 100^\circ,\ 120^\circ,\ 135^\circ,\ 150^\circ,\ 180^\circ$.
(5b). Same as (5a), but for the ratio $|B/T[W_L]|$.
(5c). Comparison of the W_L-amplitude (solid lines) and the corresponding GB-amplitude (non-solid lines) for $\theta = 10^\circ,\ 45^\circ,\ 100^\circ,\ 150^\circ$. (Here, $B[150^\circ]$ denotes the B-term at $\theta = 150^\circ$.)

Table 1. Estimates of amplitudes for $W^{\pm}W^{\pm} \to W^{\pm}W^{\pm}$ scattering.

Table 1a. Model-independent contributions from $\mathcal{L}_G + \mathcal{L}_F + \mathcal{L}^{(2)}$.

$\mathcal{L}_G + \mathcal{L}_F + \mathcal{L}^{(2)}$	$T_\ell[4\pi]$	$T_\ell[3\pi, W_T]$	$T_\ell[2\pi, 2W_T]$	$T_\ell[\pi, 3W_T]$	$T_\ell[4W_T]$
Tree-Level ($\ell = 0$)	$\frac{E^2}{f_\pi^2}$	$g\frac{E}{f_\pi}$	g^2	$e^2 g \frac{f_\pi}{E}$	g^2
One-Loop ($\ell = 1$)	$\frac{E^2}{f_\pi^2}\frac{E^2}{\Lambda^2}$	$g\frac{E}{f_\pi}\frac{E^2}{\Lambda^2}$	$g^2\frac{E^2}{\Lambda^2}$	$g^3\frac{f_\pi E}{\Lambda^2}$	$g^4\frac{f_\pi^2}{\Lambda^2}$

Table 1b. Model-dependent contributions from the next-to-leading-order effective operators.

Table 2. Order estimates of B-terms for $W^{\pm}W^{\pm} \to W^{\pm}W^{\pm}$ scattering.

Table 2a. Model-independent contributions.

$\mathcal{L}_G + \mathcal{L}_F + \mathcal{L}^{(2)}$	$B_\ell^{(0)}$	$B_\ell^{(1)}$	$B_\ell^{(2)}$	$B_\ell^{(3)}$
Tree-Level ($\ell = 0$)	g^2	$g^2 \frac{M_W}{E}$	$e^2 \frac{M_W^2}{E^2}$	$g^2 \frac{M_W}{E}$
One-Loop ($\ell = 1$)	$g^2 \frac{E^2}{\Lambda^2}$	$g^3 \frac{E f_\pi}{\Lambda^2}$	$g^4 \frac{f_\pi^2}{\Lambda^2}$	$g^4 \frac{f_\pi^2}{\Lambda^2} \frac{M_W}{E}$

Table 2b. Relevant operators for model-dependent contributions.[a]

$O(g^2 \frac{E^2}{\Lambda^2})$ (from $B_1^{(0)}$)	$O(g^3 \frac{E f_\pi}{\Lambda^2})$ (from $B_1^{(1)}$)	$O(g^2 \frac{f_\pi^2}{\Lambda^2})$ (from $B_1^{(0)}$)	$O(g^4 \frac{f_\pi^2}{\Lambda^2})$ (from $B_1^{(2)}$ or $B_1^{(0)}$)
$\mathcal{L}_{3,4,5,9,11,12}$	$\mathcal{L}_{2,3,4,5,8,9,11,12,14}$	$\mathcal{L}^{(2)\prime}$	$\mathcal{L}_{1\sim5,8,9,11\sim14}$ $(B_1^{(2)})$ $\mathcal{L}_{1,2,8,13,14}$ $(B_1^{(0)})$ $\mathcal{L}_{2\sim5,8,9,11,12,14}$ $(B_1^{(0)})$ [b]

Table 3. Global classification of sensitivities to probing direct and indirect EWSB information from effective operators at the level of S-matrix elements. [a]

Required Precision	Relevant Operators	Relevant Amplitudes	MI or MD [b] ?
$O(\frac{E^2}{f_\pi^2})$	$\mathcal{L}_0$ $(\equiv \mathcal{L}_G + \mathcal{L}_F + \mathcal{L}^{(2)})$	$T_0[4V_L] (\neq T_0[4Z_L])$	MI
$O(\frac{E^2}{f_\pi^2}\frac{E^2}{\Lambda^2},\ g\frac{E}{f_\pi})$	$\mathcal{L}_{4,5}$	$T_1[4V_L]$	MD
	$\mathcal{L}_{6,7}$	$T_1[2Z_L, 2W_L],\ T_1[4Z_L]$	MD
	$\mathcal{L}_{10}$	$T_1[4Z_L]$	MD
	$\mathcal{L}_0$	$T_0[3V_L, V_T]$ $(\neq T_0[3Z_L, Z_T])$	MI
	$\mathcal{L}_0$	$T_1[4V_L]$	MI
$O(g\frac{E}{f_\pi}\frac{E^2}{\Lambda^2},\ g^2)$	$\mathcal{L}_{3,4,5,9,11,12}$	$T_1[3W_L, W_T]$	MD
	$\mathcal{L}_{2,3,4,5,6,7,9,11,12}$	$T_1[2W_L, Z_L, Z_T],\ T_1[2Z_L, W_L, W_T]$	MD
	$\mathcal{L}_{3,4,5,6,7,10}$	$T_1[3Z_L, Z_T]$	MD
	$\mathcal{L}_0$	$T_0[2V_L, 2V_T],\ T_0[4V_T]$ [c]	MI
	$\mathcal{L}_0$	$T_1[3V_L, V_T]$	MI
	$\mathcal{L}_0$	$B_0^{(0)} \simeq T_0[3\pi, v]$ $(\neq T_0[3\pi^0, v^0])$	MI
$O(\frac{E^2}{\Lambda^2})$	$\mathcal{L}^{(2)\prime}$	$T_1[4W_L],\ T_1[2W_L, 2Z_L]$	MD
$O(g^2\frac{E^2}{\Lambda^2},\ g^3\frac{f_\pi}{E})$	$\mathcal{L}_0$	$T_0[V_L, 3V_T], T_1[2V_L, 2V_T], B_0^{(1,3)}$ [c,d]	MI
	$\mathcal{L}_{2,3}$	$T_1[4W_L]$	MD
	$\mathcal{L}_{3,11,12}$	$T_1[2Z_L, 2W_L]$	MD
	$\mathcal{L}_{2,3,4,5,8,9,11,12,14}$	$T_1[2W_L, 2W_T]$	MD
	$\mathcal{L}_{1\sim9,11\sim14}$	$T_1[2V_L, 2V_T]$ [e]	MD
	$\mathcal{L}_{4,5,6,7,10}$	$T_1[2Z_L, 2Z_T]$	MD
	$\mathcal{L}_{0,2,3,4,5,6,7,9\sim12}$	$B_1^{(0)} \simeq T_1[3\pi, v]$ [f,g]	MI + MD
$O(g^3\frac{Ef_\pi}{\Lambda^2})$	$\mathcal{L}_{0,1,2,3,8,9,11\sim14}$	$T_1[V_L, 3V_T]$ $(\neq T_1[Z_L, 3Z_T])$	MI+MD
	$\mathcal{L}_{4,5}$	$T_1[V_L, 3V_T]$	MD
	$\mathcal{L}_{6,7,10}$	$T_1[V_L, 3V_T]$ $(\neq T_1[W_L, 3W_T])$ [g]	MD
	$\mathcal{L}_{2\sim5,8,9,11,12,14}$	$B_1^{(1)} \simeq T_1[2\pi, V_T, v]$	MD
$O((g^2, g^4)\frac{f_\pi^2}{\Lambda^2})$	$\mathcal{L}^{(2)\prime}$	$T_1[2V_L, 2V_T], B_1^{(0)} \simeq T_1[3\pi, v]$ [c]	MD
	$\mathcal{L}_1$	$T_1[2W_L, 2W_T]$ [h]	MD
	$\mathcal{L}_{0,1\sim5,8,9,11\sim14}$	$T_1[4W_T]$	MI+MD
	$\mathcal{L}_{0,1\sim9,11\sim14}$	$T_1[4V_T]$ $(\neq T_1[4W_T], T_1[4Z_T])$	MI+MD
	$\mathcal{L}_{0,1,4,5,6,7,10}$	$T_1[4Z_T]$	MI+MD
	$\mathcal{L}_{1,2,8,13,14}$	$B_1^{(0)} \simeq T_1[3\pi, v]$ [c,i]	MD
	$\mathcal{L}_{0,1\sim9,11\sim14}$	$B_1^{(0)} \simeq T_1[2\pi, 2v]$ [c,j]	MI+MD
	$\mathcal{L}_{0,4,5,6,7,10}$	$B_1^{(0)} \simeq T_1[2\pi, 2v] (\neq T_1[2\pi^\pm, 2v^\pm])$ [g]	MI+MD
	$\mathcal{L}_{0,1\sim5,8,9,11\sim14}$	$B_1^{(2)} \simeq T_1[\pi^\pm, 2W_T, v^\pm]$	MI+MD
	$\mathcal{L}_{0,1\sim9,11\sim14}$	$B_1^{(2)} \neq T_1[\pi^\pm, 2W_T, v^\pm], T_1[\pi^0, 2Z_T, v^0]$	MI+MD
	$\mathcal{L}_{0,4,5,6,7,10}$	$B_1^{(2)} \simeq T_1[\pi^0, 2Z_T, v^0]$	MI+MD

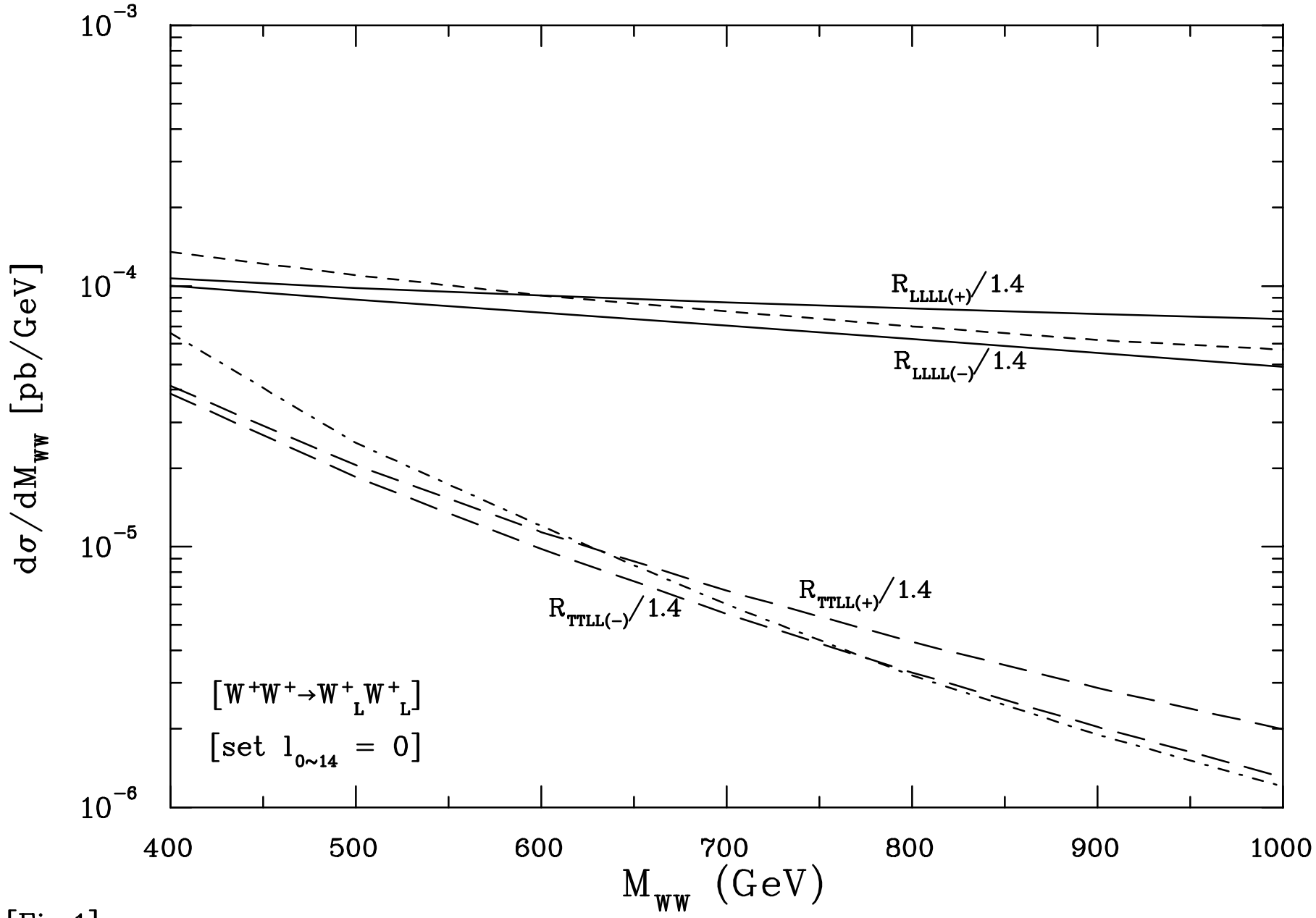
10^{-3}
10^{-4}
10^{-5}
10^{-6}
$d\sigma/dM_{WW}$ [pb/GeV]
$R_{LLLL(+)}/1.4$
$R_{LLLL(-)}/1.4$
$R_{TTLL(+)}/1.4$
$R_{TTLL(-)}/1.4$
$[W^+W^+ \to W^+_L W^+_L]$
[set $l_{0\sim14} = 0$]
400
500
600
700
800
900
1000
M_{WW} (GeV)

[Fig.1]

Table 1b. Model-dependent contributions from the next-to-leading order effective operators.

Operators	$\mathcal{L}^{(2)\prime}$	$\mathcal{L}_{1,13}$	$\mathcal{L}_2$	$\mathcal{L}_3$	$\mathcal{L}_{4,5}$	$\mathcal{L}_{6,7,10}$	$\mathcal{L}_{8,14}$	$\mathcal{L}_9$	$\mathcal{L}_{11,12}$
$T_1[4\pi]$	$\ell_0\ \frac{E^2}{\Lambda^2}$	/	$\ell_2\ e^2\frac{E^2}{\Lambda^2}$	$\ell_3\ g^2\frac{E^2}{\Lambda^2}$	$\ell_{4,5}\ \frac{E^2}{f_\pi^2}\frac{E^2}{\Lambda^2}$	/	/	$\ell_9\ g^2\frac{E^2}{\Lambda^2}$	/
$T_1[3\pi, W_T]$	$\ell_0\ g\frac{f_\pi E}{\Lambda^2}$	$\ell_{1,13}\ e^2 g\frac{f_\pi E}{\Lambda^2}$	$\ell_2\ e^2 g\frac{f_\pi E}{\Lambda^2}$	$\ell_3\ g\frac{E}{f_\pi}\frac{E^2}{\Lambda^2}$	$\ell_{4,5}\ g\frac{E}{f_\pi}\frac{E^2}{\Lambda^2}$	/	$\ell_{8,14}\ g^3\frac{f_\pi E}{\Lambda^2}$	$\ell_9\ g\frac{E}{f_\pi}\frac{E^2}{\Lambda^2}$	$\ell_{11,12}\ g\frac{E}{f_\pi}\frac{E^2}{\Lambda^2}$
$T_1[2\pi, 2W_T]$	$\ell_0\ g^2\frac{f_\pi^2}{\Lambda^2}$	$\ell_{1,13}\ e^4\frac{f_\pi^2}{\Lambda^2}$	$\ell_2\ e^2\frac{E^2}{\Lambda^2}$	$\ell_3\ g^2\frac{E^2}{\Lambda^2}$	$\ell_{4,5}\ g^2\frac{E^2}{\Lambda^2}$	/	$\ell_{8,14}\ g^2\frac{E^2}{\Lambda^2}$	$\ell_9\ g^2\frac{E^2}{\Lambda^2}$	$\ell_{11,12}\ g^2\frac{E^2}{\Lambda^2}$
$T_1[\pi, 3W_T]$	$\ell_0\ g^3\frac{f_\pi^3}{E\Lambda^2}$	$\ell_{1,13}\ e^2 g\frac{f_\pi E}{\Lambda^2}$	$\ell_2\ e^2 g\frac{f_\pi E}{\Lambda^2}$	$\ell_3\ g^3\frac{f_\pi E}{\Lambda^2}$	$\ell_{4,5}\ g^3\frac{f_\pi E}{\Lambda^2}$	/	$\ell_{8,14}\ g^3\frac{f_\pi E}{\Lambda^2}$	$\ell_9\ g^3\frac{f_\pi E}{\Lambda^2}$	$\ell_{11,12}\ g^3\frac{f_\pi E}{\Lambda^2}$
$T_1[4W_T]$	/	$\ell_{1,13}\ e^2 g^2\frac{f_\pi^2}{\Lambda^2}$	$\ell_2\ e^2 g^2\frac{f_\pi^2}{\Lambda^2}$	$\ell_3\ g^4\frac{f_\pi^2}{\Lambda^2}$	$\ell_{4,5}\ g^4\frac{f_\pi^2}{\Lambda^2}$	/	$\ell_{8,14}\ g^4\frac{f_\pi^2}{\Lambda^2}$	$\ell_9\ g^4\frac{f_\pi^2}{\Lambda^2}$	$\ell_{11,12}\ g^4\frac{f_\pi^2}{\Lambda^2}$

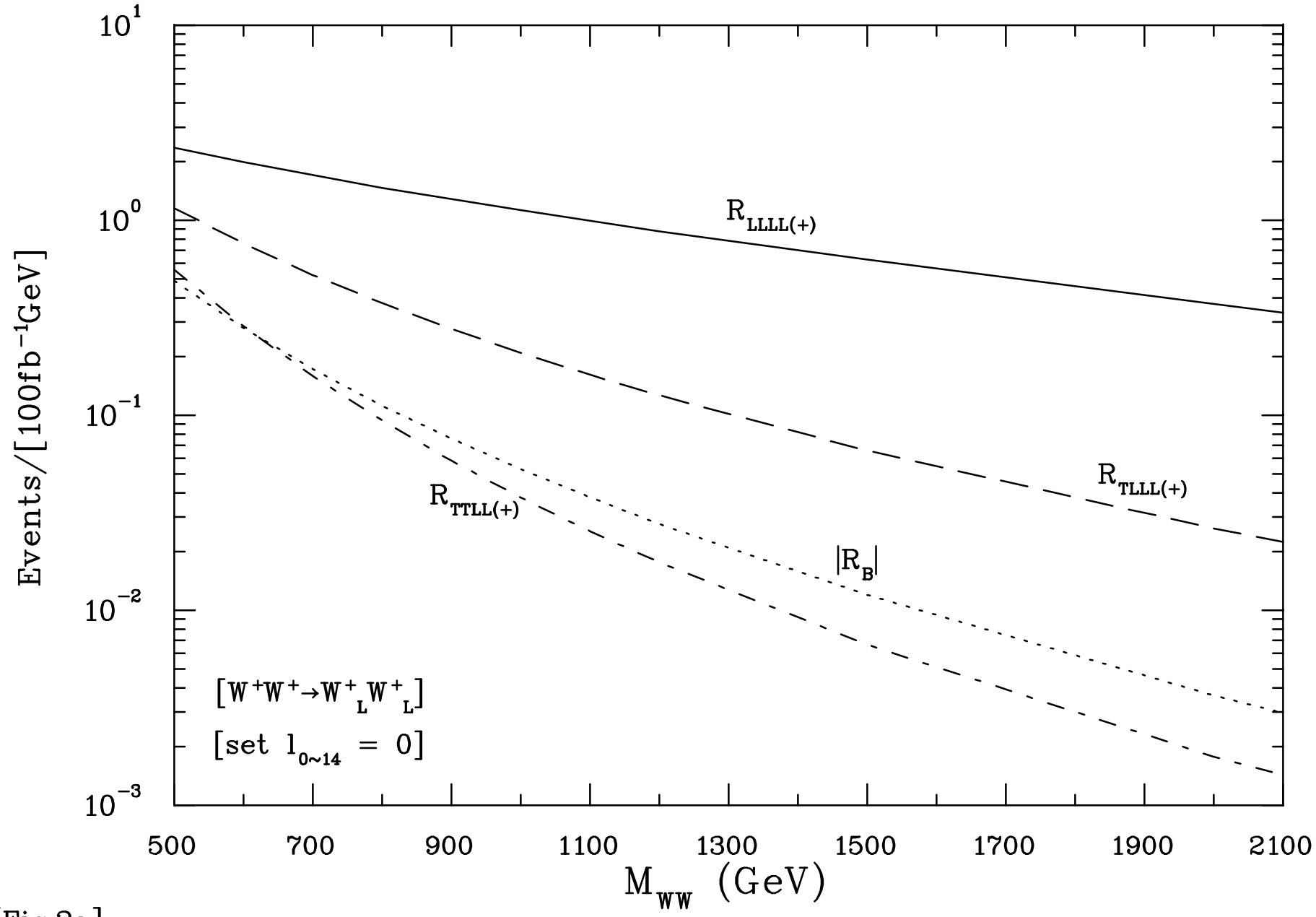
10^1
10^0
10^{-1}
10^{-2}
10^{-3}
Events/[100fb^{-1}GeV]
$R_{LLLL(+)}$
$R_{TLLL(+)}$
$R_{TTLL(+)}$
$|R_B|$
[$W^+W^+ \to W^+_L W^+_L$]
[set $l_{0\sim14} = 0$]
500
700
900
1100
1300
1500
1700
1900
2100
M_{WW} (GeV)

[Fig.2a]

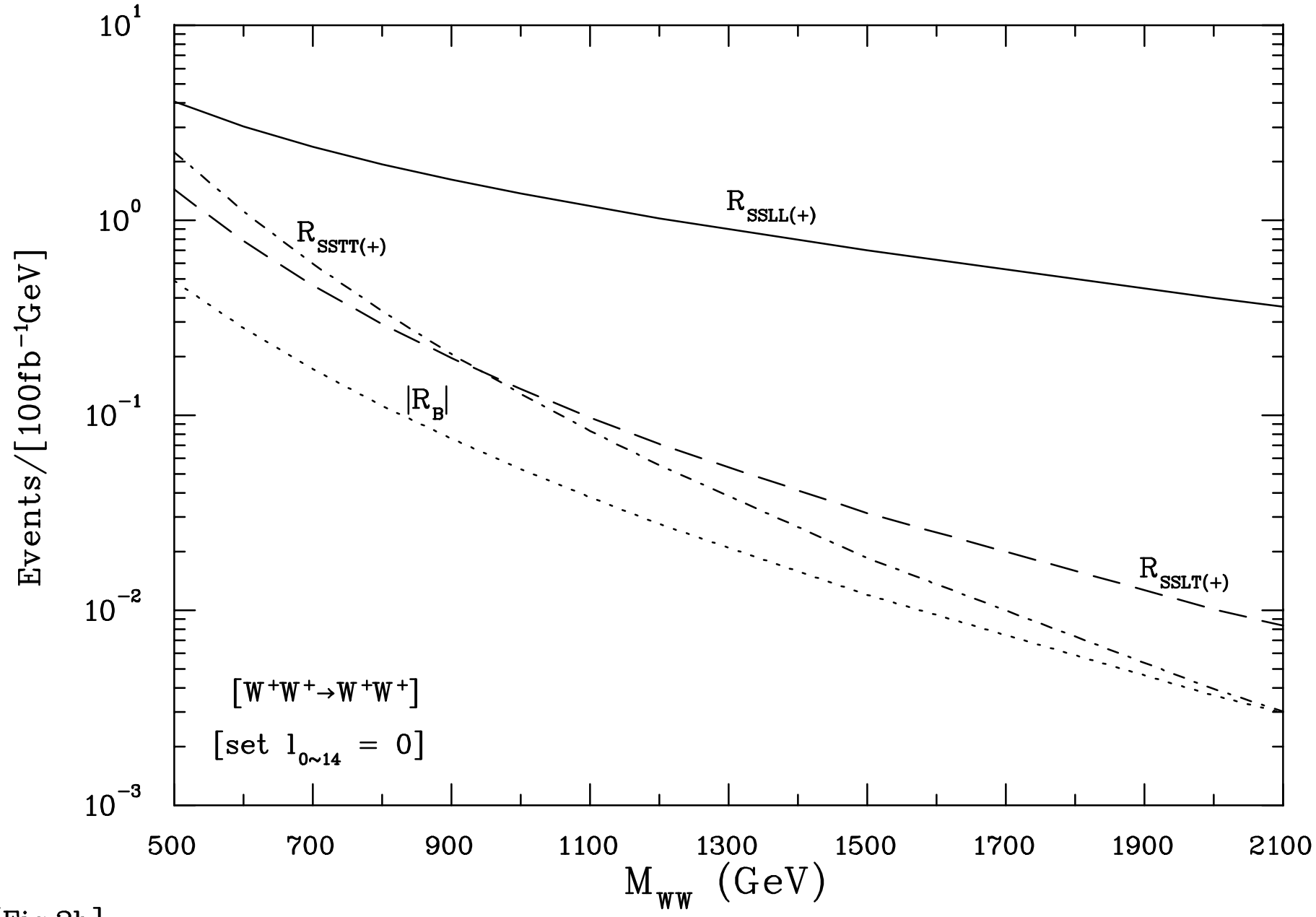
10^1
10^0
10^{-1}
10^{-2}
10^{-3}
Events/[100fb^{-1}GeV]
$R_{SSLL(+)}$
$R_{SSTT(+)}$
$|R_B|$
$R_{SSLT(+)}$
[$W^+W^+\to W^+W^+$]
[set $l_{0\sim14}$ = 0]
500
700
900
1100
1300
1500
1700
1900
2100
M_{WW} (GeV)

[Fig.2b]

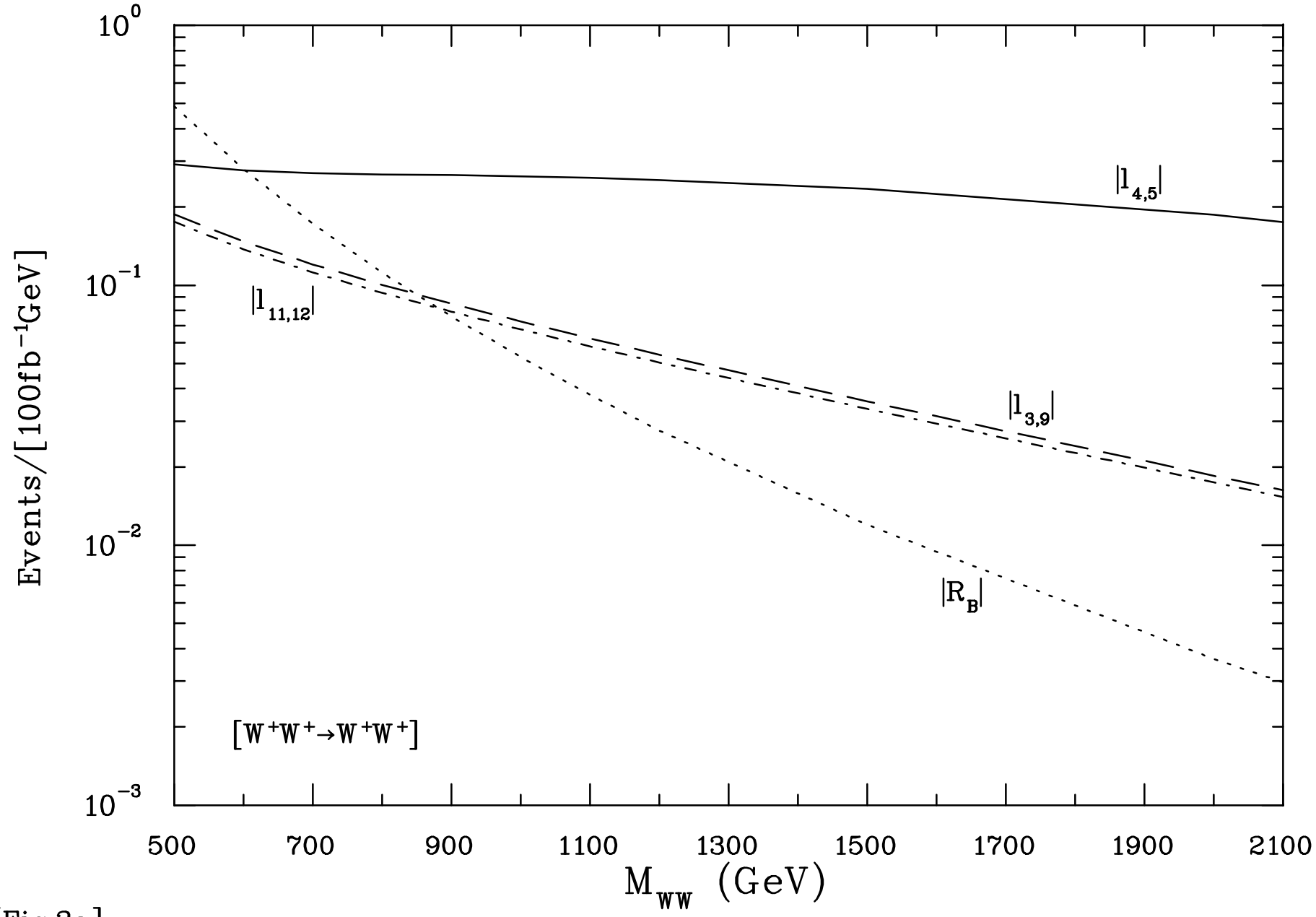
10^0
10^{-1}
10^{-2}
10^{-3}
Events/[100fb^{-1}GeV]
$|l_{4,5}|$
$|l_{11,12}|$
$|l_{3,9}|$
$|R_B|$
[$W^+W^+ \to W^+W^+$]
500
700
900
1100
1300
1500
1700
1900
2100
M_{WW} (GeV)

[Fig.3a]

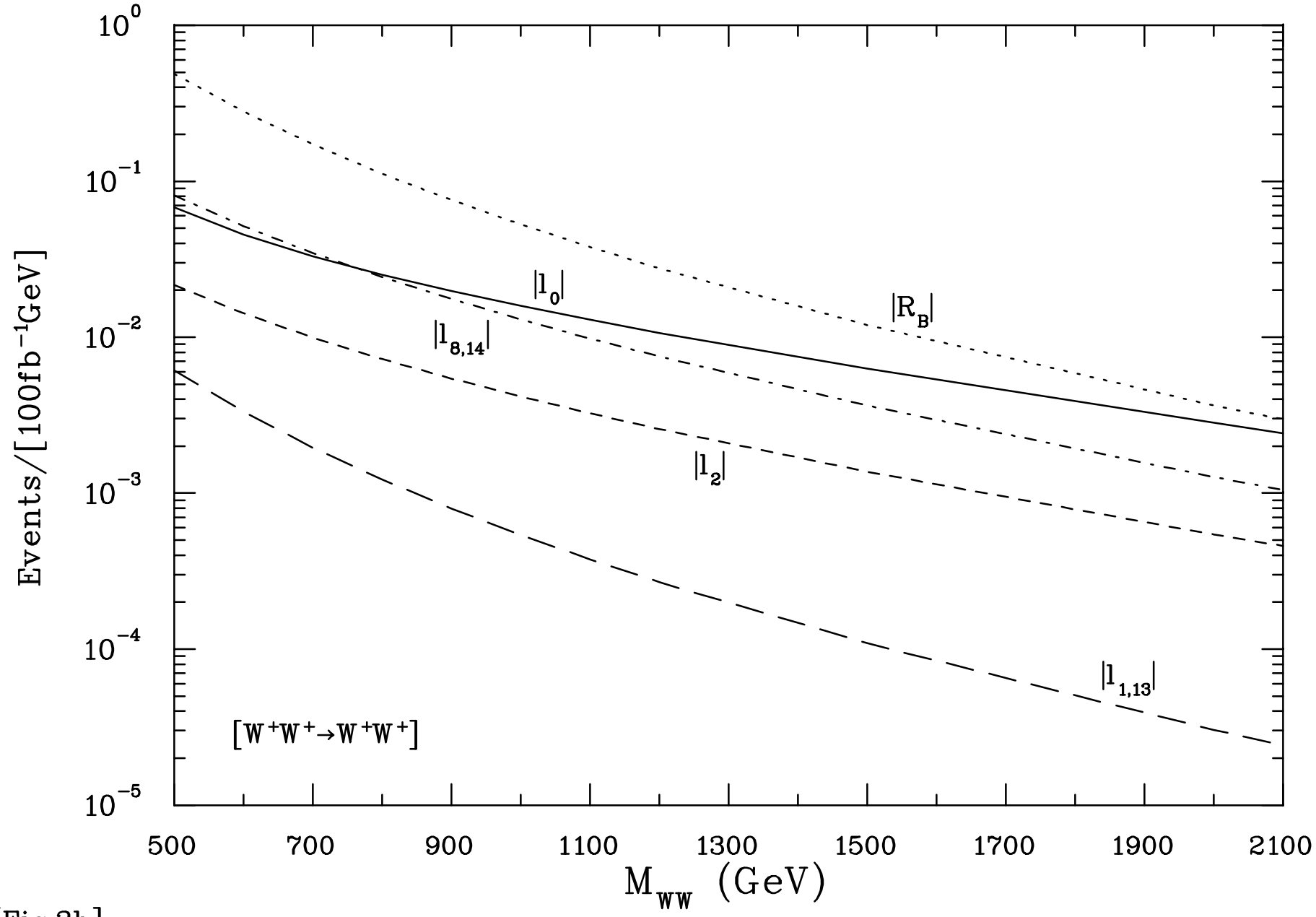
Events/[100fb^{-1}GeV]
10^{0}
10^{-1}
10^{-2}
10^{-3}
10^{-4}
10^{-5}
500
700
900
1100
1300
1500
1700
1900
2100
M_{WW} (GeV)
$|l_0|$
$|R_B|$
$|l_{8,14}|$
$|l_2|$
$|l_{1,13}|$
[$W^+W^+ \to W^+W^+$]

[Fig.3b]

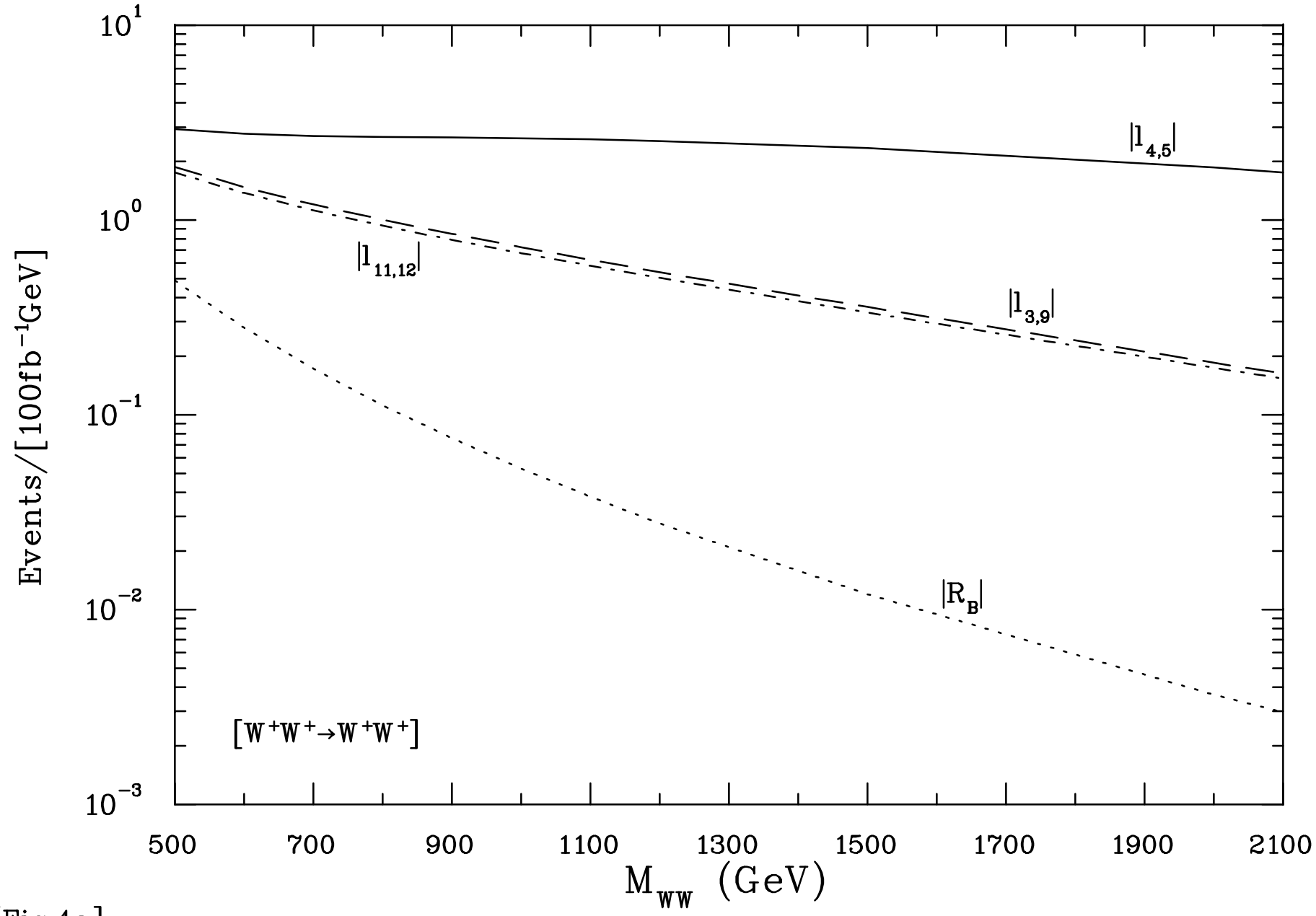
10^1
10^0
10^{-1}
10^{-2}
10^{-3}
Events/[100fb^{-1}GeV]
$|l_{4,5}|$
$|l_{11,12}|$
$|l_{3,9}|$
$|R_B|$
[$W^+W^+ \to W^+W^+$]
500
700
900
1100
1300
1500
1700
1900
2100
M_{WW} (GeV)

[Fig.4a]

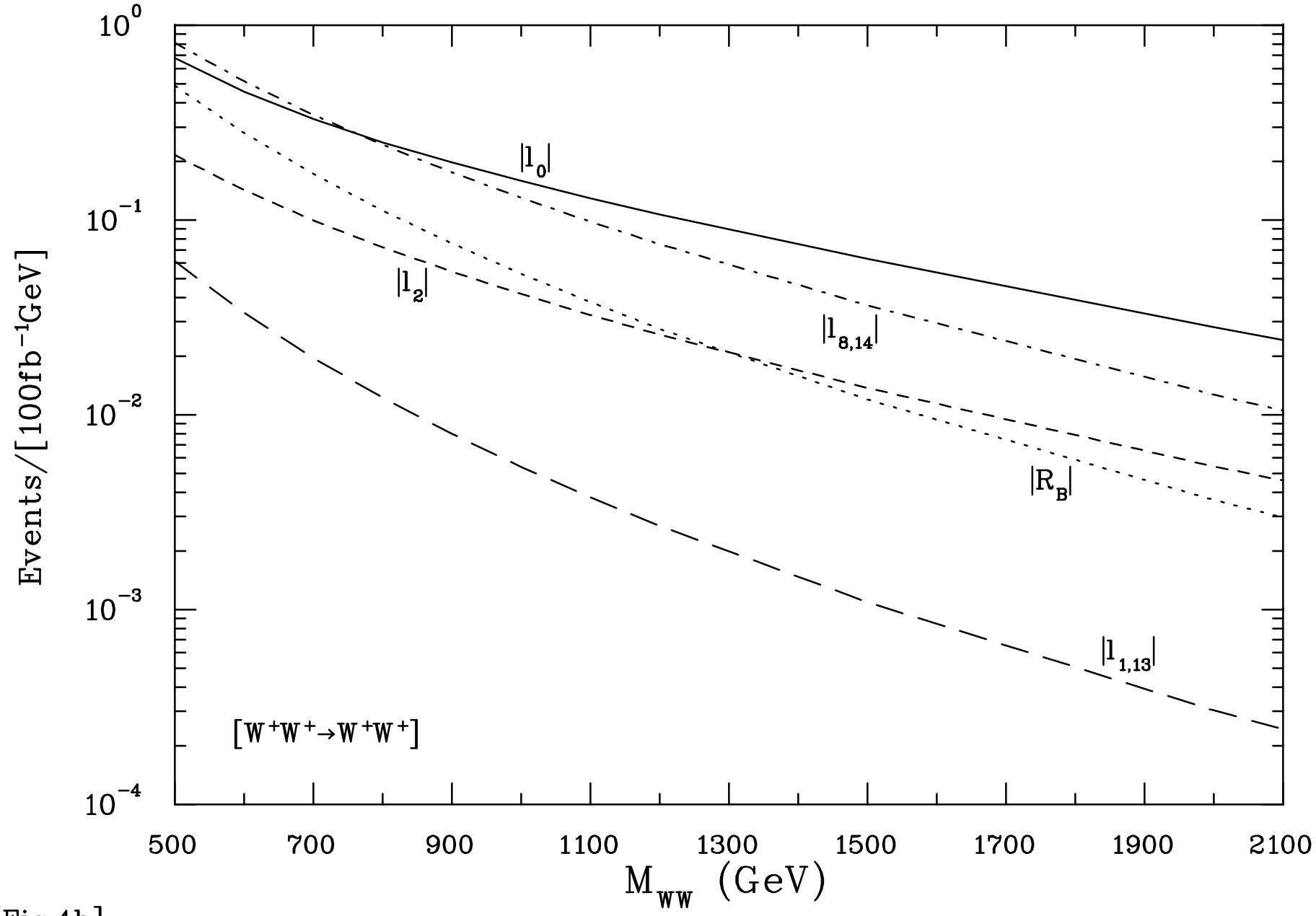
10^0
10^{-1}
10^{-2}
10^{-3}
10^{-4}
Events/[100fb^{-1}GeV]
$|l_0|$
$|l_2|$
$|l_{8,14}|$
$|R_B|$
$|l_{1,13}|$
[$W^+W^+ \to W^+W^+$]
500
700
900
1100
1300
1500
1700
1900
2100
M_{WW} (GeV)

[Fig.4b]

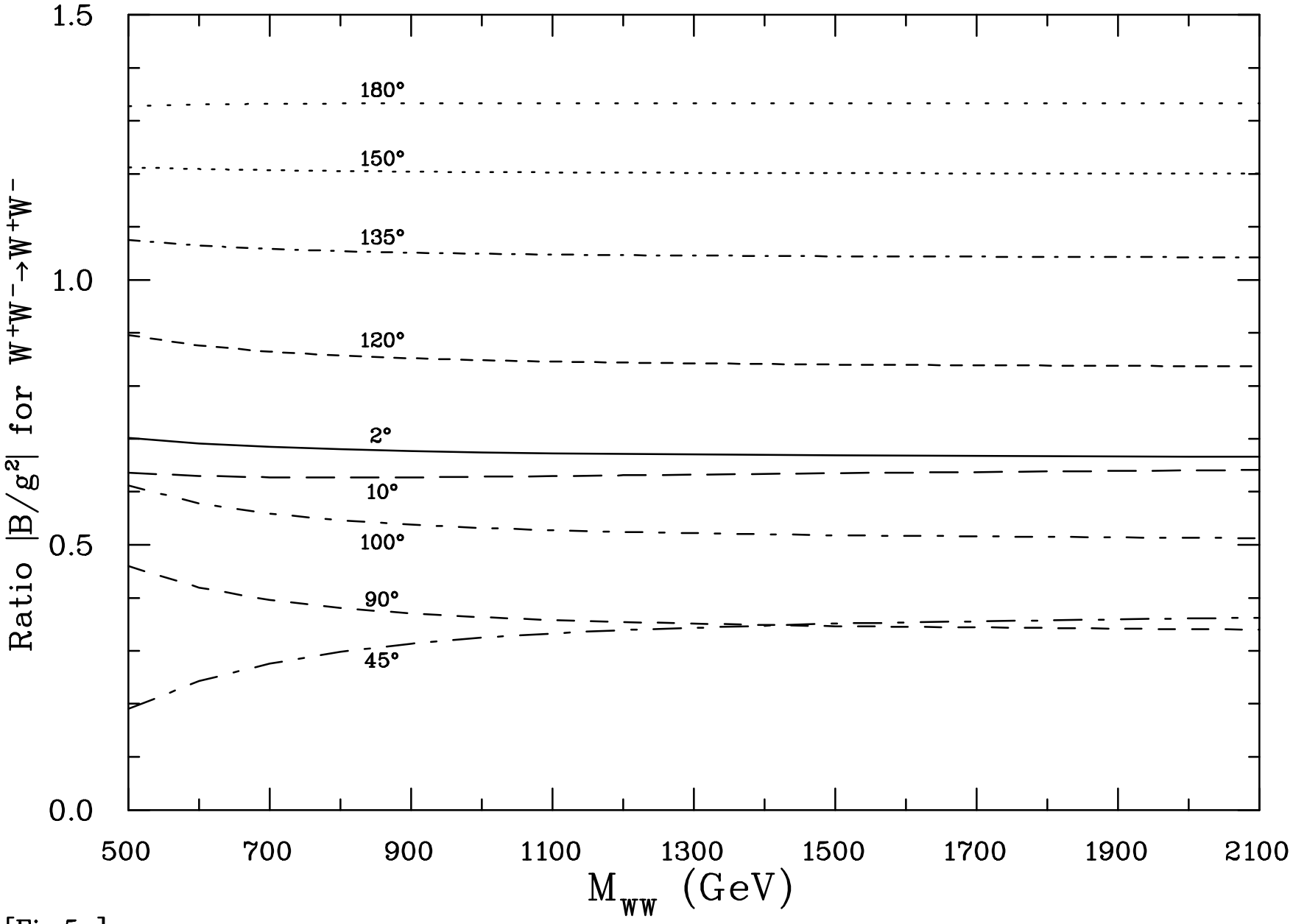
1.5
1.0
0.5
0.0
Ratio |B/g²| for W⁺W⁻→W⁺W⁻
180°
150°
135°
120°
2°
10°
100°
90°
45°
500
700
900
1100
1300
1500
1700
1900
2100
M_WW (GeV)

[Fig.5a]

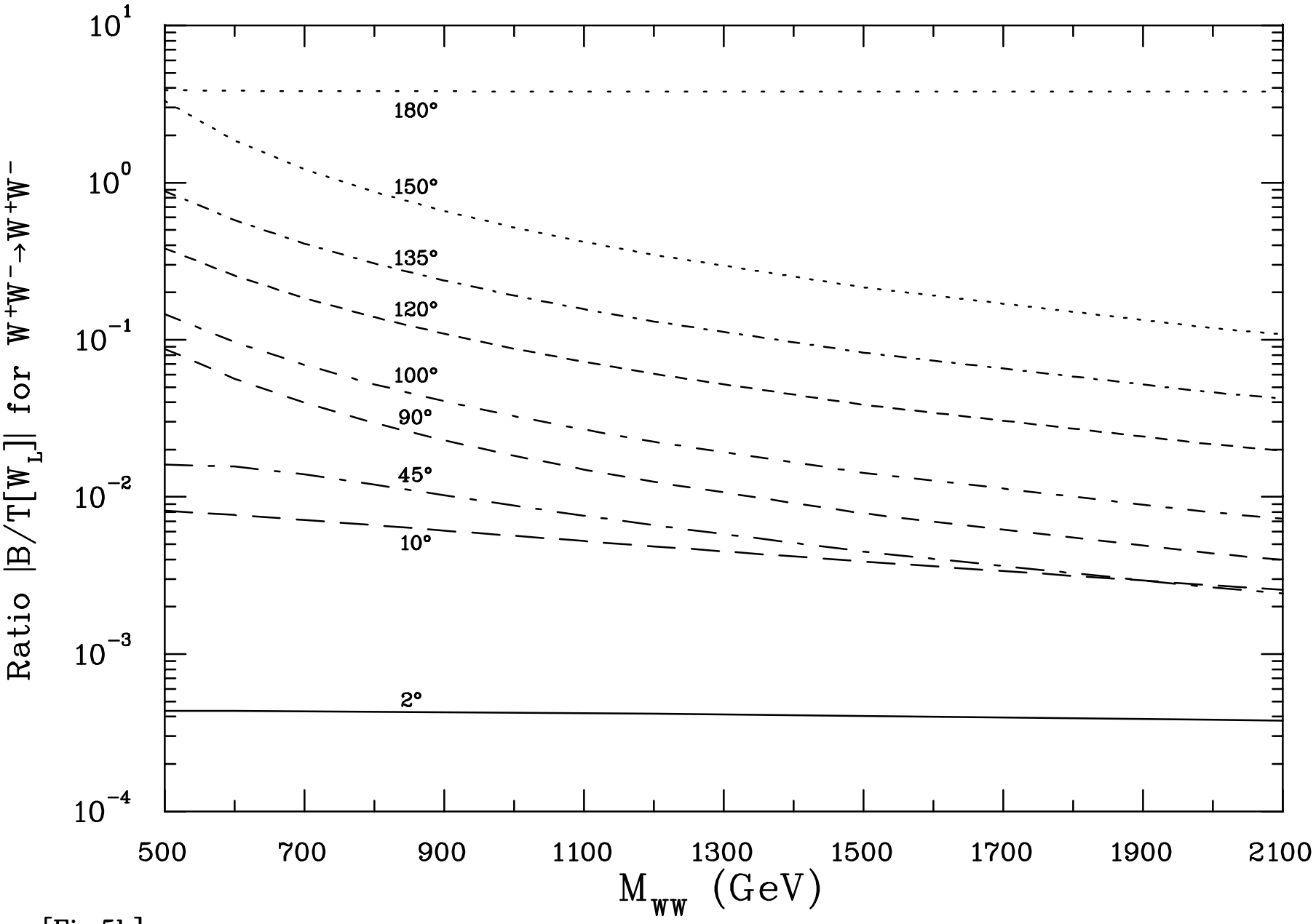
Ratio |B/T[W_L]| for W+W−→W+W−
10^1
10^0
10^−1
10^−2
10^−3
10^−4
180°
150°
135°
120°
100°
90°
45°
10°
2°
500
700
900
1100
1300
1500
1700
1900
2100
M_WW (GeV)

[Fig.5b]

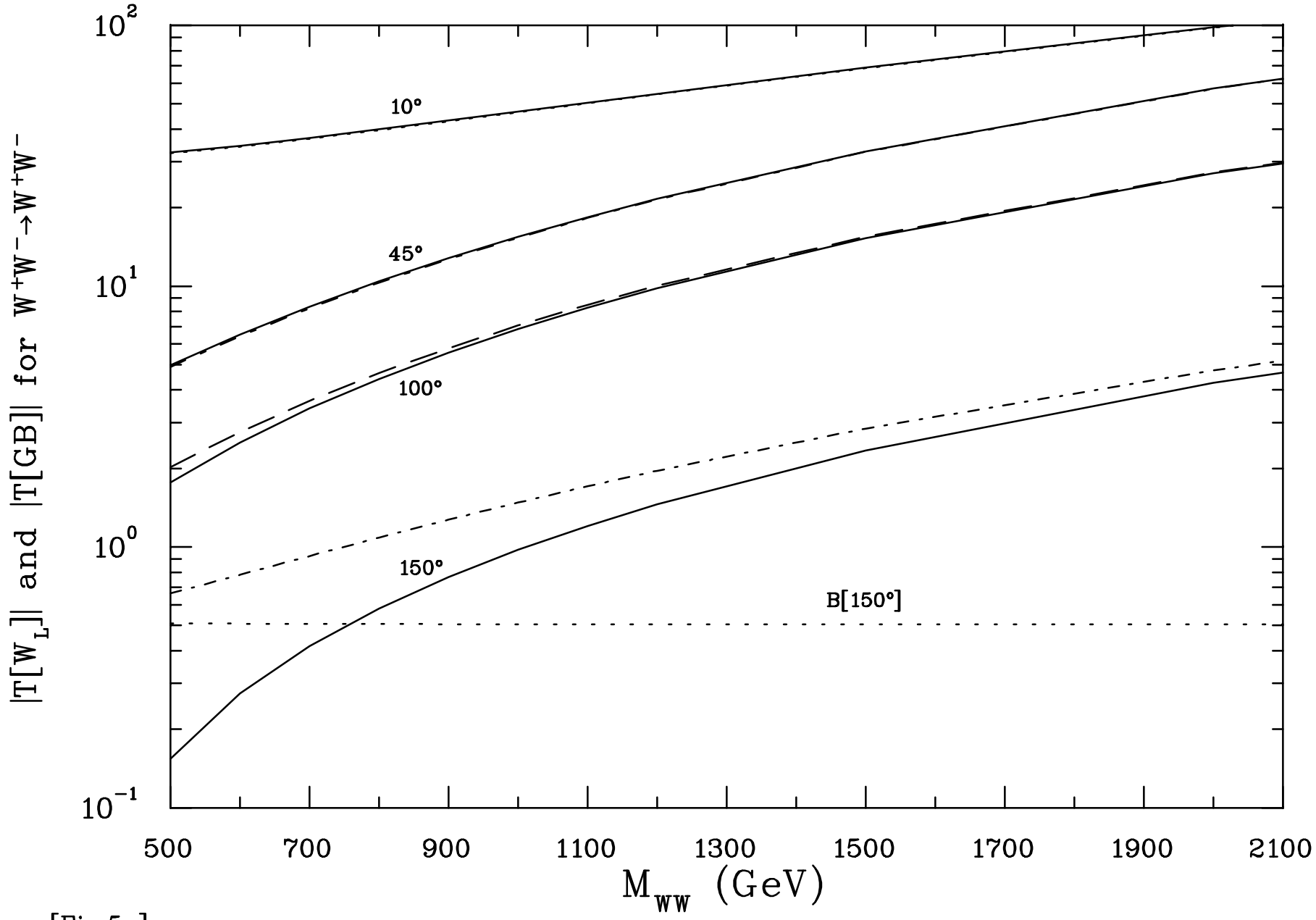
10^2
10^1
10^0
10^{-1}
$|T[W_L]|$ and $|T[GB]|$ for $W^+W^- \to W^+W^-$
10°
45°
100°
150°
B[150°]
500
700
900
1100
1300
1500
1700
1900
2100
M_{WW} (GeV)

[Fig.5c]